



Sapienza University of Rome

ARCHMAT

**(Erasmus Mundus Joint Master in Archaeological Materials
Science)**

Scienze e Tecnologie per la Conservazione dei Beni Culturali

"Study of the Most Effective Analysis Procedures Using Multispectral
Imaging Techniques on Ancient Egyptian Painted Objects"

Islam Shaheen

1903096

Relator:

Prof. Stefano Ridolfi

Sapienza University

Rome, December 2020



SAPIENZA
UNIVERSITÀ DI ROMA



ARISTOTLE
UNIVERSITY
OF THESSALONIKI



UNIVERSIDADE DE ÉVORA

Dedication

(In memory of my Father)

My humble efforts I dedicate to

My lovely Mother & My sweet wife

*Whose affection, love, encouragement and prays make me able to get such
success and honor,*

Along with all hard working and respected Teachers.

Acknowledgments

The completion of this study could not been possible without the expertise of Prof. Stefano Ridolfi (Head of Research Department of Ars mensurae), my thesis Supervisor.

A debt of gratitude is also owed to

Prof. Nicola Schiavon (coordinator of the consortium of ARCHMAT),

Prof. Evangelia Varella (coordinator of Aristotle University of Thessaloniki),

Prof Donatella Magri and Prof. Gabriele Favero (coordinators of Sapienza University of Rome),

And all of the professors and staff in Evora, Aristotle and Sapienza universities for their great assistance and support.

Special thanks to Prof. Mie Ishii (Associate Professor, Saga University) and

Ms. Akiko Nishisaka (GEM-JC Project Manager)

For providing the MSI equipment used in this study.

Abstract

Multispectral imaging (MSI) used as Initial studies to identify and study painted layers as a non-destructive method. The use of MSI to tentatively identify pigments has an important advantage justifying its application the rapid and low-cost survey of large areas.it is possible to tentatively identify some historical pigments and discover the invisible layers, painting and writing. By means of MSI performed with simplified equipment and without the aid of imaging analysis software.

The two selected objects from the Grand Egyptian Museum collection were rich in pigments, first object is polychrome anthropoid wooden coffin lid (*GEM No. 22452*) the date back to 21st Dynasty (c. 1070 - 945 B.c.) Late period, which belong to the collection of Bab el-Gusus tomb and the second is a Cartonnage mummy trappings on linen (*GEM No. 8615*) date back to 27th dynasty, late period.

Different imaging techniques of multispectral imaging like ultraviolet methods (UVF, UVR, and UVRFC) and Infrared methods (IRF, IR, IRFC and IRT) will be studied and evaluated regarding to the efficiency and effectively. Mixing between multispectral imaging and Reflectance transformation imaging will be applied and tested by mix and match between these two techniques we can add value for the results we can get. Several methods will be applied practically to have the required results for evaluating these methods. X-ray fluorescence (XRF) spectrometry was used as a complementary analysis for the identification of the pigments.

Keywords

Multispectral Imaging, Reflectance Transformation Imaging, Cartonnage, Coffin, X-Ray Fluorescence, Pigments, Ancient Egypt.

Table of Contents

Dedication	I
Acknowledgments	II
Abstract	III
Keywords	III
Table of Contents	IV
List of Figures	VIII
List of Charts	XI
List of Tables	XII
Introduction	XIII
Chapter One: State of Art	1
1. Pigments in Ancient Egypt	2
2. Electromagnetic Spectrum	3
2.1. Ultraviolet Spectrum.....	3
2.2. X-Rays.....	3
2.3. Infrared Spectrum.....	4
3. Multi-Spectral Imaging	4
Chapter Two: Materials	6
Object Case Studies	7
1. Case Study 1: Wooden Coffin Lid (GEM No. 22452).....	7
2. Case Study 2: Cartonnage Mummy Trappings (GEM No. 8615).....	11
Chapter Three: Methodology	12
1. Introduction	13
2. Multispectral Imaging Methods	13
2.1. VIS photography.....	13
2.2. Ultraviolet Imaging.....	14
2.2.1. Two types of UV were applied in this study.....	15

2.2.1.1. UVF (UV Fluorescence).....	15
2.2.1.2. UVR (UV Reflected).....	15
2.2.2. Tools.....	15
2.2.2.1. Camera.....	15
2.2.2.2. Lenses.....	16
2.2.2.3. Light Source.....	16
2.2.2.4. Filters.....	17
2.2.3. Procedures for UV Imaging.....	17
2.2.3.1. Ultraviolet Fluoresce UVF.....	17
2.2.3.2. Ultraviolet Reflected UVR.....	17
2.3. Infrared Imaging.....	18
2.3.1. Five Techniques of IR Were Applied.....	18
2.3.1.1. Infrared (IR).....	18
2.3.1.2. Infrared Fluorescence (IRF).....	18
2.3.1.3. False Color (IRFC).....	19
2.3.1.4. IR Transmitted.....	19
2.3.1.5. IRFC Transmitted.....	19
2.3.2. Tools.....	19
2.3.2.1. Camera.....	19
2.3.2.2. Lenses.....	20
2.3.2.3. Light source.....	20
2.3.2.4. Filters.....	20
2.3.3. Procedures of IR Imaging.....	21
2.3.3.1. Infrared Imaging.....	21
2.3.3.2. Infrared Florescence (IRF).....	21
2.3.3.3. Infrared False Color (IRFC).....	21
2.3.3.4. IR Transmitted.....	21

2.3.3.5. IRFC Transmitted.	22
3. Reflectance Transformation Imaging (RTI).	23
3.1. Two Types of RTI Were Applied.	24
3.1.1. RTI VIS.	24
3.1.2. RTI IR.	24
3.2. Tools.	24
3.2.1. Camera.	24
3.2.2. Lenses.	24
3.2.3. Light Source.	24
3.2.4. Spheres.	24
3.2.5. Software.	25
3.3. Procedures of RTI Imaging.	25
3.3.1. RTI VIS.	25
3.3.2. RTI IR.	26
4. X-ray Radiography.	27
5. X-Ray Fluorescence (XRF) Analysis.	28
5.1. Analysis's Devices.	28
6. Digital Microscope (VHX-950F Series).	29
Chapter Four: Results 31	31
1. Case Study 1: Wooden Coffin Lid (GEM No. 22452).	32
1.1. Ultraviolet Florescence.	33
1.2. Infrared Florescence.	35
1.3. Infrared False Color (IRFC).	36
1.4. Infrared.	37
1.5. X- Ray Radiography.	38
1.6. Reflectance Transformation Imaging (RTI).	40
1.7. X-ray Fluorescence (XRF) Analysis for the Painted Layers.	43

1.7.1. Yellow Painted Layer.....	43
1.7.2. Blue Painted Layer.....	46
1.7.3. Green Painted Layer.....	47
1.7.4. Red Painted Layer.....	50
1.7.5. Black	52
2. Case Study 2: Cartonnage Mummy Trappings (GEM No. 8615)	53
2.1. Ultraviolet Fluorescence (UVF)	54
2.2. Ultraviolet Reflected (UVR).....	55
2.3. Ultraviolet Reflected False Color (UVRFC)	57
2.4. Infrared IR.....	57
2.5. Infrared Fluorescence IRF	58
2.6. Infrared Fluorescence False Color (IRFFC)	59
2.7. Infrared False Color(IRFC).....	59
2.8. Visible Transmission	60
2.9. IR Transmitted	60
2.10. IRFC Transmitted	61
2.11. Reflectance Transformation Imaging (RTI) (VIS RTI – IR RTI)	62
2.12. X-ray Fluorescence (XRF) Analysis.....	67
2.12.1. Yellow Painted Layer.....	68
2.12.2. Blue Painted Layer.....	69
2.12.3. Green painted layer	71
2.12.4. Red Painted Layer.....	72
2.12.5. White Painted Layer.....	74
Chapter Five: Discussion.....	75
Chapter Six: Conclusion.....	83
Bibliography	86

List of Figures

Figure 1. The Electromagnetic Spectrum (photo by NASA Science).....	4
Figure 2. Bab El-Gusus Tomb entrance. Photo source: Metropolitan Museum of Art.....	7
Figure 3. Egypt Map Showing Bab El-Gusus Tomb Location.....	8
Figure 4. Plan of the Tomb with the Original Position of the Burial Sets.....	9
Figure 5. Wooden Coffin Lid 21st Dynasty (C. 1070 - 945 B.C.).....	10
Figure 6. Cartonnage Mummy Trappings on Linen.....	11
Figure 7. NIKON D810. Photo source: https://www.nikon.com/	15
Figure 8. Lenses Nikon 60mm and Tokina 35mm.....	16
Figure 9. UV LED lamb.....	16
Figure 10. Filters left: IDAS UV 390 middle: Baader UV/IR- cut/ L Right: IDAS VLC 31.....	17
Figure 11. Toshiba LDR9N-W - near IR K- light illuminator LED.....	20
Figure 12. IDAS IR830 52mm.....	20
Figure 13. IR Transmitted setup.....	22
Figure 14. Spheres.....	24
Figure 15. RTI Builder & Viewer Software.....	25
Figure 16. RTI setup for RTI IR.....	26
Figure 17. Cuattro Slate Cesium-I Detector System.....	27
Figure 18. Niton™ XL3t GOLDD hand held XRF spectrophotometer.....	28
Figure 19. Digital Microscope VHX-950F Series.....	29
Figure 20. Coffin full image from left A-Visible – B-UVF – C-IRF – D-IR.....	32
Figure 21. UV details of the chest and middle part of the coffin.....	34
Figure 22. UV clear details showing the retouches of previous treatment.....	34
Figure 23. Details of IRF showing different in blue color.....	35
Figure 24. Clear details.....	36
Figure 25. Left: visible and IRFC in the middle – on the right IR.....	36
Figure 26. Details IRFC.....	37
Figure 27. Details of IR.....	37
Figure 28. X-Ray radiography.....	38
Figure 29. Details showing ornamental figures represented by the scarab and the sun (Up) and the ear which appears in coarse paste (Down).....	39

Figure 30. RTI Details of Coffin. A – Visible B- Diffuse gain C- Specular enhancement D- Normal visualization.....	41
Figure 31. Details of the grainy surface of the yellow painted layer.....	42
Figure 32. Details of black lines.....	42
Figure 33. Different methods of MSI were applied.....	53
Figure 34. UV Fluorescence.....	54
Figure 35. Details of UVF.....	55
Figure 36. Details of UVF.....	55
Figure 37. from left: Visible light photo – UVR photo – UVRFC photo.....	56
Figure 38. Infrared photo.....	57
Figure 39. IRF details shows the Egyptian blue.....	58
Figure 40. Infrared Fluorescence false color - Infrared false color.....	59
Figure 41. Details shows the yellow, Red and green pigments in the IRFC.....	60
Figure 42. Visible Transmissin - IR Transmitted - IRFC Transmitted.....	61
Figure 43. RTI VIS with different filters (Diffuse Gain – Specular Enhancement – Normal Visualization).....	63
Figure 44. RTI IR with different filters (Diffuse Gain – Specular Enhancement – Normal Visualization).....	63
Figure 45. The diffuse gain filter shows the grainy surface of the yellow layer and the preparation layer.....	64
Figure 46. Details with different filters: A: default – B: specular enhancement – C: normal unsharp masking – D: normal visualization.....	64
Figure 47. Details with different filters for Visible RTI: A: default – B: Diffuse Gain– C: specular enhancement – D: normal visualization and RTI IR filters E: default – F: Diffuse Gain– G: specular enhancement – H: normal visualization.....	65
Figure 48. Eight spots of XRF.....	67
Figure 49. UV photo shows the conservation materials and additional touches.....	75
Figure 50. UV photo cotton swabs and the remains of fabric material on the surface of the Cartonnage.....	76
Figure 51. UVR the white color which indicator for gypsum.....	76
Figure 52. IRFC show the lighter blue and red as indication of malachite and Egyptian blue.	77

Figure 53.UVRFC, IRFC give indicator for red color.....	77
Figure 54. Grains of Green pigments under microscope.....	77
Figure 55. UVRFC, IRFC give indicator for yellow color.....	78
Figure 56.IRFC , IRF show Egyptian blue mapping.....	78
Figure 57. RTI photos: left specular enhancement filter, right diffuse gain filter.....	79
Figure 58. IR RTI: left specular enhancement filter, right diffuse gain filter.....	80
Figure 59. RTI: diffuse gain filter shows the preparation layer texture.....	81
Figure 60. RTI photo specular enhancement show the sequence of adding the figures and pigments.....	82

List of Charts

Chart 1. Yellow pigment chart.....	43
Chart 2. Chart of yellow pigment.	44
Chart 3. Blue pigment chart.....	46
Chart 4. Chart of Blue pigment.....	46
Chart 5. Green pigment chart.....	48
Chart 6. Chart of Green pigment.....	48
Chart 7. Red pigment chart.	50
Chart 8. Chart of Red pigment.....	51
Chart 9. Chart of yellow pigment.	68
Chart 10. Chart of Blue pigment.....	69
Chart 11. Chart of blue pigment	70
Chart 12. Chart of green pigment.	71
Chart 13. The results of X-ray fluorescence (XRF) for the Red layers.	73
Chart 14. Chart of white layer.....	74

List of Tables

Table 1. Summary of the different methods which were used in the Methodology.....	30
Table 2. The results of X-ray fluorescence (XRF) for the yellow color.....	45
Table 3. The results of X-ray fluorescence (XRF) for the yellow color.....	45
Table 4. The results of X-ray fluorescence (XRF) for the blue color.....	47
Table 5. The results of X-ray fluorescence (XRF) for the Green color.....	49
Table 6. The results of X-ray fluorescence (XRF) for the Green color.....	49
Table 7. The results of X-ray fluorescence (XRF) for the Green color.....	50
Table 8. The results of X-ray fluorescence (XRF) for the Red color.	52
Table 9. The results of X-ray fluorescence (XRF) for the yellow layers.	69
Table 10. The results of X-ray fluorescence (XRF) for the Blue layers.....	70
Table 11. The results of X-ray fluorescence (XRF) for the Green layers.....	72
Table 12. The results of X-ray fluorescence (XRF) for the Red layers.....	73
Table 13. The results of X-ray fluorescence (XRF) for the white layers.	74

Introduction

The research aims to enhance the documentation of cultural work through the use of advanced and emerging technologies. These technologies create new ways of documentation. The objectives of the research are to develop and promote digital technology for documenting artifacts for conservation; and to promote the development and use of new or advanced techniques for documentation. The careful study of the surface topography of cultural work is a critical component to understanding and protecting the object as a whole. The research presents an overview of the usefulness of Multispectral imaging, combined with elemental analysis method, in better understanding cultural work and will address what types of documentation projects it best supports. Focusing on objects in the Grand Egyptian Museum (GEM) collection that were documented using Multispectral imaging technology and elemental analysis method using X-ray fluorescence, with this research, I try to provide a broad understanding of how this technology can influence better understanding on objects materials and technique.

The objectives for applying these digital and computational imaging techniques help in documenting the current condition before and after conservation treatment, build an integrated, comprehensive, high-resolution data set using non-invasive techniques. These techniques also aid in the selection of areas for further testing and analysis using complementary methods. Allow detailed correlation of further analytical tests and imaging data with spectral, spatial/geometric, and textural features and examining the changes in composition and areas of damage, and to distinguish original pigments from later conserving.

Visual examination and documentation of a culturally important object can provide valuable information which needed study and discover the history. However, sometimes important details about an object may not be visible to the naked eye by using visible light. This is where other regions of the electromagnetic spectrum can provide more information about surface properties and also about what lies beneath the surface. Multispectral imaging (Infrared, ultraviolet), X-ray and γ -ray radiation can be utilized (Stuart, 2007).

Two objects from the Grand Egyptian Museum were chosen for this study: the ancient Egyptian polychrome anthropoid wooden coffin lid and cartonnage mummy trappings on linen.

The inner structures of painted layers for these two objects are investigated to gain insight into the artistic process, painting techniques, and pigments, to detect previous conservation treatments and also to determine the best conditions for preservation. Non-invasive analytical methods such as multispectral imaging methods were used in this study. Multispectral imaging performs a non-invasive identification of several colorants, causing no damage or mechanical stress to the objects subjected to analysis.

The spectral features of the colorants along with the benefits of extending the spectral range of analysis, can be best appreciated as a rapid preliminary tool that offers an overview on the main colorants employed and guides the selection of painted areas of objects on which more selective techniques, such as X-ray fluorescence, can be employed for a more complete and accurate identification.

Chapter One: State of Art

Chapter Contents:

- **1. Pigments in Ancient Egypt.**
- **2. Electromagnetic Spectrum.**
 - **2.1. Ultraviolet Spectrum.**
 - **2.2. X-rays.**
 - **2.3. Infrared Spectrum.**
- **3. Multi-Spectral Imaging.**

1. Pigments in Ancient Egypt.

The pigments used by ancient Egyptians considered the most diverse pigment palette of the ancient world. The identification of ancient Egyptian pigments usually aggravated by chemical interactions between pigment and binder media or between the pigment and environmental pollutants or both. Colors to Egyptians were not just the value or scarcity of the materials that mattered but the symbolic meaning of the colors and the beauty of the image that they could construct from it and were intended to convey meaning and imbue an image with greater power.

The word “iwn” (color) also translates as “disposition”, “character”, “complexion” and “nature”, confirming that color was seen as being intimately linked to the essence of being. The ancient Egyptian palette was formed around six main color groups: green (wadj); red (desher); blue (irtyu or khesbedj); yellow (khenet or kenit); white (hedj or shesep); and black (kem).

The Egyptian artist had six colors including black and white. These colors were generated from mineral compounds and thus retain their vibrancy over the millennia. For example, the reds and yellows from ochre containing iron oxides; some reds from realgar, a sulfide of arsenic (AsS), red ochre or hematite for red; yellow ochre for yellow; blue and green from azurite and malachite; blue from atacamite, hydrated copper chloride ($\text{Cu}_2\text{Cl}(\text{OH})_3$), Egyptian blue was a synthetic pigment created mainly from copper silica and calcium; green from malachite (a natural copper ore) or, then, from a paste manufactured by mixing oxides of copper and iron with silica and calcium; bright yellow, representing gold, from orpiment, another sulfide of arsenic (As_2S_3); pale yellow from jarosites, a mineral containing sulfates of iron and potassium ($\text{KFe}_3(\text{OH})_6(\text{SO}_4)_2$) and black was made of carbon compounds (soot, ground charcoal, and animal bones). Color is to be distinguished from pigments, the organic or inorganic coloring substance. Egyptian pigments before the Roman period are in most instances inorganic substance, explaining the extraordinarily good preservation of color on many Egyptian antiquities and monuments.

2. Electromagnetic Spectrum.

Expands from high-energy (frequency) gamma rays to low-energy (frequency) radio waves. Note that the visible region is only a tiny region of the spectrum. (Ebbing et al., 2012) Visible light has wavelengths ranging from 400 nm (violet) to 780 nm (red). The colors we see with our eyes in our day to day lives have wavelengths between this 400-780 nm (Holler et al., 1999). On the left and right of the visible range there are UV range and IR range which using in multispectral imaging (Fig 1).

2.1. Ultraviolet Spectrum.

UV Spectrum – moving forward to the left of the visible region would lie the ultraviolet region. Although not visible to the naked eye, this region would appear to be violet as it is nearer to the violet region of the visible spectrum and hence the name ultraviolet spectrum. It lies between the ranges of 10 nm to 380 nm.

2.2. X-Rays.

Going to the left of the ultraviolet spectrum, there is first the X-rays (0.01 nm to 10 nm). Hard X-rays have shorter wavelengths than soft X-rays and as they can pass through many substances with small absorption, they can be used to 'see through' materials with 'thicknesses' less than that equal to a few meters of water (NASA Science). One notable use is diagnostic X-ray imaging in cultural heritage especially with coffins and mummies (a process known as radiography).

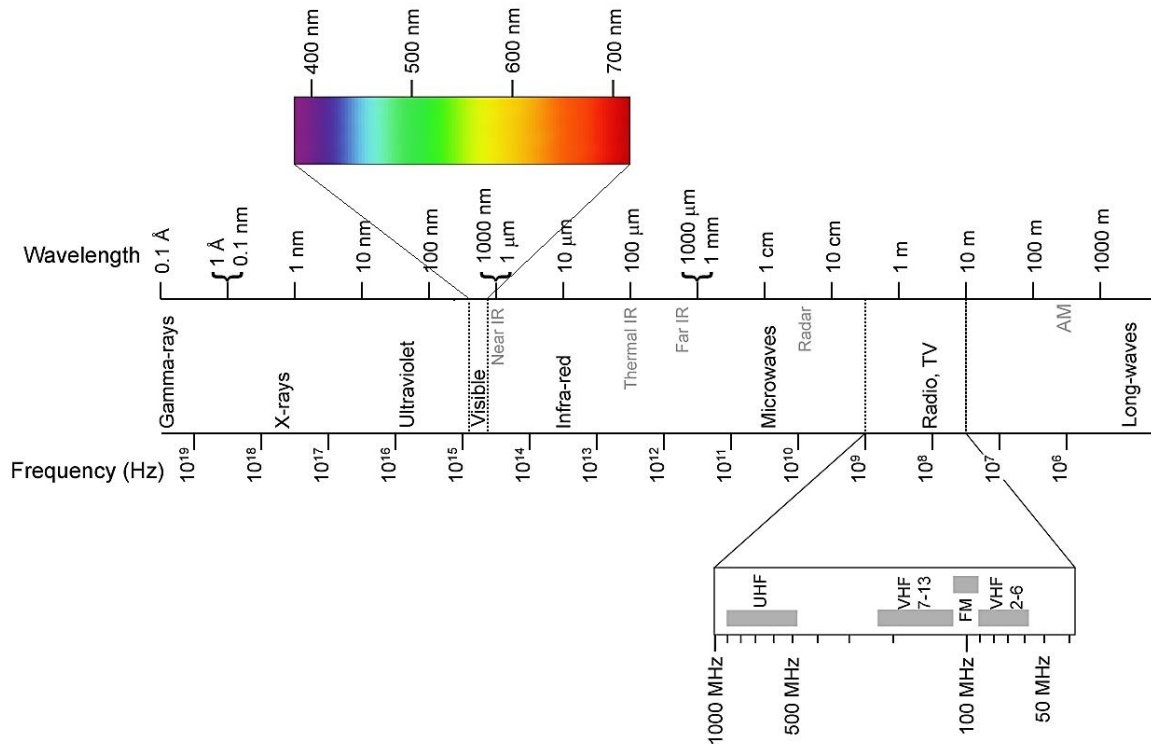


Figure 1. The Electromagnetic Spectrum (photo by NASA Science).

2.3. Infrared Spectrum.

IR Spectrum – to the right of the visible region, there would lie the infrared spectrum region. The first discovery of electromagnetic radiation other than visible light was in 1800, when William Herschel discovered infrared radiation. Similar to the UV spectrum, the infrared spectrum is invisible to the naked eye, however since the region is nearer to the red region of the visible spectrum, it is known as the infrared region. The wavelength range lies between 780nm to 1mm. (Douglas et al., 2003).

3. Multi-Spectral Imaging.

Multispectral imaging measures the reflectance and fluorescence properties of the pigments using different wavelengths of light within the ultraviolet (UV), visible, and near-infrared (IR) spectrum.

It is one of the most important techniques in cultural heritage studies. This importance came from being one of the non-destructive scientific methods, which is considered as a first measure to tentatively identify some historical pigments and discover the invisible layers, painting and

writing, detect some marks of tools used in the application of the pigments or used in making artifacts, the presence of any conservation process or newly applied materials on the antiquities, identification of artists materials, and determining their spatial distribution in artwork all this information will be used after that in the study plan and for the maintenance of cultural heritage. Multispectral imaging (MSI) techniques are getting used more and more often by conservators and conservation scientists these techniques are getting popular in this field because they're simple, affordable, lightweight, and small. Sampling on important pieces of art isn't possible and this is often the most reason why only non-invasive techniques, like MSI, are getting increasingly popular to help with undertaking conservation decisions (Antonino, 2015). Also, it has the advantage of being a preference for application in the archaeological site or laboratories, as it is considered one of the measures that can be performed in different circumstances commensurate with the nature of the impact.

The use of MSI to tentatively identify pigments features a significant advantage justifying its application the rapid and low-cost survey of huge areas. MSI is performed with simplified equipment and without the aid of imaging analysis software However, there are procedures that are followed to apply these techniques, which follow some steps, and some differences in their application may affect a difference or defect in the expected results of these techniques. In this study, the different procedures for applying multispectral imaging techniques are discussed to recognize the most effective analysis procedures for the cultural heritage studying that enable us to obtain the best results. Mixing between multispectral imaging and other imaging techniques like RTI (reflectance transformation imaging) are applied and tested too by mix and match between these two techniques we can add value for the results we can get. Different imaging techniques will be studied and evaluated regarding to the efficiency and effectively.

One of the most important points is choosing the archaeological material that will be applied to this study. Some pieces rich in pigments were selected from the ancient Egyptian collection, which was and still is a rich area for research and study, with a variety of pigments and different methods of application and that was found in a wooden coffin and a piece of cartonnage. These pieces, because of the painting layers they contain, are suitable for the study and evaluation of the imaging methods.

Chapter Two: Materials

Chapter Contents:

- **Object Case Studies.**

- 1. Case Study 1: Wooden Coffin Lid.**

- 2. Case Study 2: Cartonnage Mummy Trappings.**

Object Case Studies.

Two case studies are discussed from the Grand Egyptian Museum collection.

Object Name / Description	Polychrome Anthropoid Wooden Coffin	Cartonnage Mummy Trappings
Date	21st Dynasty (c. 1070 - 945 B.c.)	27th dynasty
Object Type	Tomb equipment	
Medium, Technique	Wood, paint	Cartonnage, linen, paint
Dimensions	186 cm - 67 cm - 25 cm	31.5 cm – 17.5 cm
Inventory Number	GEM No. 22452	GEM No. 8615
Collection	Egyptian art	Egyptian art

1. Case Study 1: Wooden Coffin Lid (GEM No. 22452).

An ancient Egyptian polychrome anthropoid wooden coffin lid (Figure. 5) belonging to late period, 21st Dynasty (c. 1070 - 945 B.c.) at the beginning of period, 21st Dynasty which the high priests of Amun assumed the rule over Egypt from the last of the Ramessides.

It was discovered 1891 in the Bab el-Gusus tomb (Figure. 4), Bab el-Gasus, also known as the tomb of the Priests of Amun, is placed outside the north-eastern corner of the Hatshepsut temple-precinct (Figure. 3). The tomb had provided excellent conditions for the preservation of the burial sets for almost 3000 years and

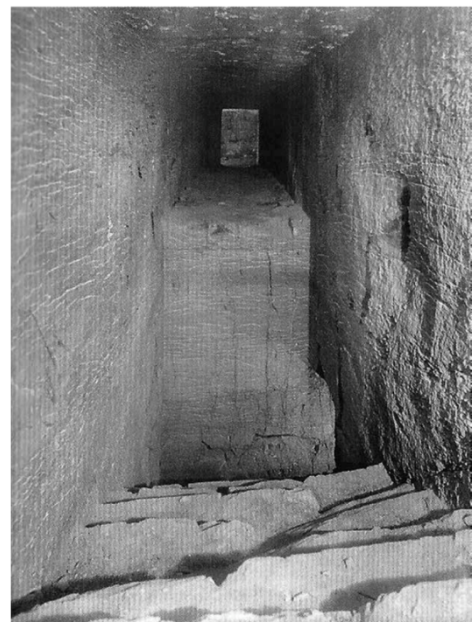


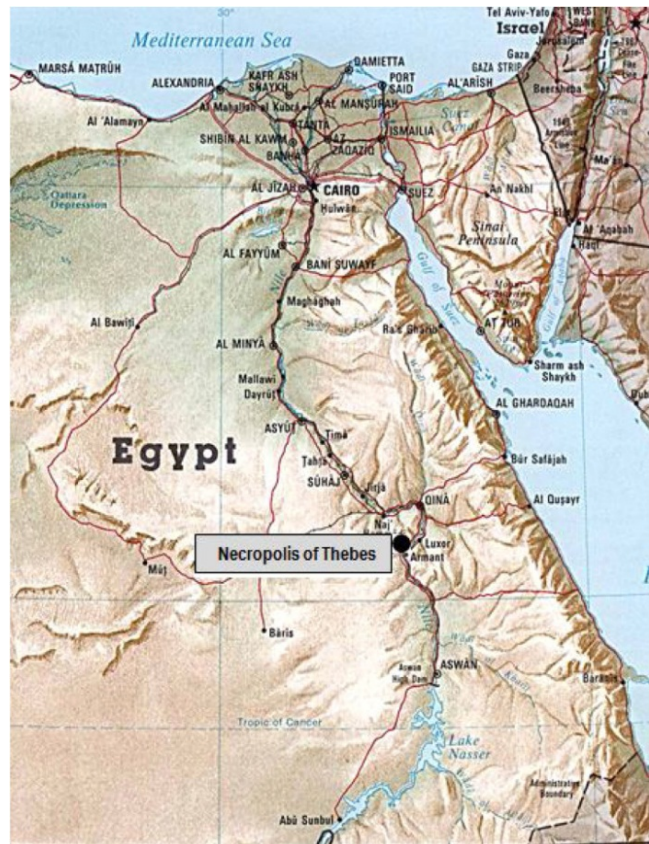
Figure 2. Bab El-Gusus Tomb entrance. Photo source: Metropolitan Museum of Art.

the objects were in perfect condition (G. Daressy, 1896). This site, the largest settled tomb ever found in Egypt, was discovered in 1891 By Eugène Grébaut and Georges Daressy, only ten years after the ‘Royal Cache’ (1881).

The reason that the tomb was not discovered earlier lies in its efficient blocking system. The entrance to the tomb had been sealed with a multi-layered system of large stones protruding from the surface and concealing an asymmetrically arranged pavement of limestone slabs.

Around 153 coffin sets buried (figure. 4) were found inside its galleries, it was still well below its storage capacity, which could have easily held at least more 70 coffin sets. The impressions registered by Daressy give a clear account of his exploration of the tomb. The doorway was opened on 4 February 1891. It showed a long undecorated corridor felled out of the rock, 1.70 to 1.90 meters wide, and of a similar height (Figure. 2) (Souza, 2018).

Figure 3. Egypt Map Showing Bab El-Gusus Tomb Location.



As one of the 153 coffins that were discovered in the tomb, and because of The stylistic heterogeneity of the coffins, the methods presented in this study and the method were applied to this coffin will provide an opportunity to present a non-destructive comparative study of the inscriptions, decorations and archaeological layers distinguished for this period of time, thus identify the use of sophisticated methods by the Theban workshops and knowledge of the artistic features of the era and the extent of progress in the industry and craftsmanship that characterize that era.



Figure 4. Plan of the Tomb with the Original Position of the Burial Sets. Drawing by Rogério Sousa.

Figure 5. Wooden Coffin
Lid 21st Dynasty (C. 1070 -
945 B.C.).



2. Case Study 2: Cartonnage Mummy Trappings (GEM No. 8615).

Cartonnage mummy trappings on linen (Figure. 6) with dimensions 31.5 cm – 17.5 cm back to late period 27th dynasty support decorated with god hours on the top to the right winged sun disk three goddesses lotus flower and rosette contains hieroglyphic text down to the winged sun disc in the middle of the piece.

As flat object made of textile and textile covered with painted layer (cartonnage) that's will help in applying more techniques and will be suitable for studying by adding different methods like IR transmitted and RTI IR.

Different techniques were applied for studying these objects, multi spectral imaging, Reflectance transformation imaging, X-ray radiography and X-ray fluoresce.



Figure 6. Cartonnage Mummy Trappings on Linen.

Chapter Three: Methodology

Chapter Contents:

- **1. Introduction.**
- **2. Multispectral Imaging Methods**
 - **2.1. VIS photography.**
 - **2.2. Ultraviolet Imaging.**
 - **2.3. Infrared Imaging**
- **3. Reflectance Transformation Imaging (RTI).**
- **4. X-ray Radiography.**
- **5. X-Ray Fluorescence (XRF) Analysis.**
- **6. Digital Microscope (VHX-950F Series).**

1. Introduction.

The research methodology, based on the data from the visual inspection under stereo microscope and technical photography and non-invasive analysis using portable elemental analysis were performed directly on differently colored areas.

The investigation is largely based on non-invasive methods of analysis thus keeping invasive measures to a minimum. The two objects were examined at the Grand Egyptian Museum (GEM). The techniques employed include Multispectral imaging, ultraviolet fluorescence (UVF) examination, visible-induced luminescence (VIL) imaging and X-ray fluorescence spectrometry (XRF)

All visual observations are supported by photographic documentation. After the preliminary examination at the museum, the painted layers were analyzed.

2. Multispectral Imaging Methods.

Multispectral imaging (MSI) measures the reflectance and fluorescence properties of the different pigments using different wavelengths of light within the ultraviolet (UV), visible (VIS), and near-infrared (IR) spectrum. Multispectral is a 12 reflected wavebands, including ultraviolet (UV), 6 visible (VIS), and 5 infrared (IR).

Low-cost multispectral imaging system used for the identification and studying objects in artworks. For getting the technical images visible light (VIS), ultraviolet fluorescence (UVF), ultraviolet reflected (UVR), visible-induced infrared luminescence (VIL) and infrared (IR), Infrared transmission (IRT), a modified digital camera was used in different spectral ranges (from 360 to about 1100nm). Two objects were photographed by different techniques; some techniques were mixed in application with other to have the ideal result of these methods.

2.1. VIS photography.

Cultural heritage investigation begins with visible photography documentation in the standard visible range of the electromagnetic spectrum (Piqué et al., 2015) Color camera

calibration, highlight correction, white balance, sharpness, focus system, color checkers, resolution. These are some of the topics to understand in order to secure quality photo documentation of art objects and archaeology. It's important also because it is the image that will be used in the comparisons between the methods presented in this study and to know how much invisible information was obtained and revealed, which was not clear to the naked eye in a visual examination.

2.2. Ultraviolet Imaging.

Ultraviolet-induced fluorescence is a commonly used technique for the characterization and identification of painting materials, such as organic binders, varnish and colorants. Its interpretation is strongly connected to both the procedures setup and an understanding of the physical and chemical interactions between materials in paint layers, which are commonly composed of a fluorescent organic binder and a pigment.

When illuminated with UV radiation, the light emitted by fluorophores present in the materials undergoes several kinds of interactions, in particular scattering and absorption by pigmented particles and auto-absorption (VERRI, 2008).

Ultraviolet (UV)-induced fluorescence is a widely exploited phenomenon in the analysis of polychrome. In particular, fluorescence spectroscopy is a noninvasive tool that can differentiate between materials with similar optical properties but different chemical compositions. Like the use of the same color for restoration and conservation processes, but it differs in chemical composition, then UV helps in detecting previous restoration processes, or other non-original materials on the surface of a work of art and identifying the authenticity of archaeological materials. Fluorescence spectroscopy can highlight the presence of retouching, coatings, varnishes and in some cases natural colorants present in wood, silk textiles, natural varnishes, painting, wall painting, ceramics and glass.

2.2.1. Two types of UV were applied in this study.

2.2.1.1. UVF (UV Fluorescence).

Comes just from the surface of the paint layer and it isn't influenced by layers below. Though in this case, the varnish layer plays a major role since it generally shows strong fluorescence and could overcome the actual fluorescence of the pigments. Consequently, sometimes MSI is recommended when the varnish is removed from the artwork.

2.2.1.2. UVR (UV Reflected).

UV light interacts just with the very surface layer of paint, therefore the UVR image is restricted to the topmost pigment and layers of paint underneath don't influence it. Furthermore, a consistent varnish coating doesn't conflict with the pigments' appearance within the UVR but it'll absorb some UV producing just a change within the overall brightness (Cosentino, 2014).

2.2.2. Tools.

2.2.2.1. Camera.

The UV images in this study were acquired with a Nikon D810 DSLR (36.3 MP FX, CMOS sensor) (Fig 7) digital camera modified for “full spectrum”, ultraviolet-visible infrared photography (between about 360 and 1100 nm). The CMOS sensor reacts both to the near-infrared and near-ultraviolet ranges of the spectrum. For commercial cameras available in the market, there is a IR cut-off filter that cuts out the infrared ray, but some companies that will remove this filter in commercial cameras for a small fee, which enables the camera is said to be “full-spectrum”. For the calibration process, The X-rite Color Checker Passport was used as a reference alongside the object.



Figure 7. NIKON D810. Photo source: <https://www.nikon.com/>

2.2.2.2. Lenses.

Tokina 35mm f/2.8 AT-X PRO DX Macro Lens for Nikon and A Nikon Nikkor 60mm f/1:2.8D AF lens were used for all the MSI photos (fig.8).



Figure 8. Lenses Nikon 60mm and Tokina 35mm. Photo source : <https://www.nikon.com/> , <https://www.bhphotovideo.com/>

2.2.2.3. Light Source.

Two portable USB UV 365nm LED lambs were used for ultraviolet (UV) (Figure.9).



Figure 9. UV LED lamb.

2.2.2.4. Filters.

IDAS UV 390 52mm – Baader UV/IR- cut/ L filter - IDAS VLC 31 52mm (Fig.10).



Figure 10. Filters left: IDAS UV 390 middle: Baader UV/IR- cut/ L Right: IDAS VLC 31.

2.2.3. Procedures for UV Imaging.

2.2.3.1. Ultraviolet Fluoresce UVF.

Some steps were followed to apply the UVF technique in dark space by using the modified camera D810 with the Tokina lens 35mm and two portable USB UV 365nm LED lamps. A combination IDAS VLC 31 52mm and Baader UV/IR- cut/ L filters were used on the lens to cut both ultraviolet reflected and the possible infrared stray radiation generated by the lamps. The camera is connected to a computer to provide sharp focusing in non-visible modes (UV) using live view mode.

2.2.3.2. Ultraviolet Reflected UVR.

IDAS UV 390 52mm filtering system was placed in front of the camera lens for the acquisition of ultraviolet reflected images (UVR) in order to block the visible component and investigate ultraviolet range. The camera should be on fully manual mode and tethered to a computer using live view mode to control the camera focus and the setting of the camera (ISO- Aperture – Shutter speed).

- (For the coffin 4 photos were taken then collected by adobe Photoshop)

2.3. Infrared Imaging.

Similar to UV, near-IR photography has been used in analyzing works of art for many decades. Some inks and pigments that are visually indistinguishable are frequently different under NIR (780–2500 nm). (Kubik, 2007).

It's helpful by classify the behavior of each pigment with respect to the IR region as transparent, reflective, or absorbent. When observing the IR image of the pigment swatches, if the pigment is IR transparent if there any carbon ink line could be distinguished, if it is IR reflective, the pigment will look bright, and therefore the ink line is going to be not visible.

IR Photography and IR Reflectography are commonly getting used in this field. Roughly, IR Photography is measuring reflection between 800nm and 1000nm while IR Reflectography can measure up to 2000nm allowing the higher revealing of strata (Boer, 1968).

Revealing of under-drawings has been noted to be clear in the IR region above 1000nm, around 1000 to 2000nm (Walmsley et al., 1992). Thus, detecting under-drawings using IR photography between 800 to 1000nm has many difficulties and limitations (El-Rifai et al., 2013).

IR Photography can be conducted in several ways; reflected, transmitted, false color, and fluorescence. The majority of literature is concentrated on the reflected IR while the IR transmitted technique is not as prominent (Moutsatsou et al., 2011).

2.3.1. Five Techniques of IR Were Applied.

2.3.1.1. Infrared (IR).

Is obtained by emitting VIS and IR radiation passing through surface layers and by using a filter to block visible wavelength to reveal under-drawings. A modified sensor required to detect some information in the Near-Infrared (NIR).

2.3.1.2. Infrared Fluorescence (IRF).

Is captured by emitting VIS light on the surface and using an IR filter to restraint some wave-length to detect chemical material with an IR fluorescence response.by using this method

Some molecules and minerals (among them mineral pigments) present Infrared Fluorescence. This phenomenon is similar to Ultraviolet Fluorescence where a beam of ultraviolet light generates visible light emission. In the case of infrared fluorescence, a beam of visible light produces an emission of infrared radiation. IRF photography allows to map and identify Egyptian blue and cadmium-based pigments.

2.3.1.3. False Color (IRFC).

Is composite images digitally computed by swapping RGB layers in between IR and VIS to link non-visible areas of interest with a visible false- color relevancy but could be also used for pigment mapping. IRFC will be used too because it is useful to identify and examine single layer paint so it will be help to know the layers of the colors if it was one or multilayers.

2.3.1.4. IR Transmitted.

Infrared Transmittance Imaging was proved to be more suitable and effective for observation of deteriorated aspects of the painting (cracks and fragile parts), because IR is partially absorbed by materials in the layers.

2.3.1.5. IRFC Transmitted.

Is composite of two images digitally computed by swapping RGB layers in between IR transmitted and VIS transmitted. Through overlaid image we can check the positions and nature of cracks.

2.3.2. Tools.

2.3.2.1. Camera.

Nikon D810 DSLR (36.3 MP FX, CMOS sensor) (fig 1).

2.3.2.2. Lenses.

Tokina 35mm f/2.8 AT-X PRO DX Macro Lens for Nikon and A Nikon Nikkor 60mm f/1:2.8D AF lens were used for all the MSI photos (fig 2).

2.3.2.3. Light source.

Two LED lamps Toshiba LDR9N-W used for IRF and near IR K- light illuminator LED Wave Length 780 - 1020nm which used as source light for IR and IR transmitted (Fig 11).



Figure 11. Toshiba LDR9N-W - near IR K- light illuminator LED.

2.3.2.4. Filters.

IDAS IR830 52mm (fig 12).



Figure 12. IDAS IR830 52mm.

2.3.3. Procedures of IR Imaging.

2.3.3.1. Infrared Imaging.

Is performed with two LED IR lamps and IDAS IR830 52mm cut-on filter was placed in front of the lens to block the visible component and investigate the range between 850 and 1000nm. This technique is used in revealing the presence of any preliminary drawings or carbon-based pigment (wills, 2012).

2.3.3.2. Infrared Florescence (IRF).

The objects were illuminated by two LED lamps Toshiba LDR9N-W and a IDAS IR830 52mm cut-on filter was placed in front of the lens, to block all stray radiations from visible spectrum and investigate only the emission of IR radiation in the 850–1000nm region. This technique was used to reveal the presence of Egyptian blue pigment that shows photo-induced luminescence properties in the infrared range (Verri et al.,2014). In the VIL images, Egyptian blue pigment shows up as bright white areas against a dark background.

2.3.3.3. Infrared False Color (IRFC).

Images are made by digitally editing and mixing the (RGB) channels of the VIS and IR images by adobe Photoshop.

2.3.3.4. IR Transmitted.

Photography has been conducted; the object was on transparent sheet of glass and IR lights were positioned on a safe distance from the back side of the cartonnage, while area camera sensitive in the range of 380 to 1100nm was facing the front side (fig 13), the visible and UV radiation have been blocked by IR filter IDAS IR830 52mm, to capture IR transmitted images in the range of 830 to 1000nm (El-Rifai 2013).

2.3.3.5. IRFC Transmitted.

Images are made by digitally editing and mixing the (RGB) channels of the VIS and IR transmitted images by adobe Photoshop.



Figure 13. IR Transmitted setup.

3. Reflectance Transformation Imaging (RTI).

RTI is a computational photographic technique that captures artifacts surface shape and color and allows the interactive re-lighting of the topic from any direction. RTI also allows the mathematical enhancement of the subject's surface shape and color properties. The enhancement functions of RTI reveal surface information that's not disclosed under direct empirical examination of the object (CHI 2002-2020).

This kind of technology has significant potential within the Cultural Heritage (CH) field, where the way light interacts with the item is vital within the 3D visual observation and study of humanity's legacy. The characteristics of the fabric, reflectance behavior, and texture offer major perceptual and cognitive hints for the study of those types of objects.

Each RTI resembles one, two-dimensional (2D) photographic image. Unlike a typical photograph, reflectance information springs from the three-dimensional (3D) shape of the image subject and encoded within the image per pixel, in order that the synthesized RTI image "knows" how the light will reflect off the subject (Malzbender et al., 2001).

RTI techniques use economical and widely available hardware in several cases, just a digital camera and light, and can easily do a sampling density and precision. Digital models encoding only the 3D shape are not able to capture all the outstanding and interesting aspects of the artwork. In many cases, the ability to interactively operate with the light is often more useful than the manipulation of an accurately sampled 3D shape (G. Palma et al. 2010). For those reasons, RTI techniques are widely used in the CH field and highly recommended as documentation tools and to support detailed visual analysis (Mudge et al., 2005].

RTI images are created from information obtained from multiple digital photographs of a subject shot from a stationary camera position. In each photograph, light is proposed from a different known, or knowable, direction. This process produces a sequence of images of the same subject with different highlights and shadows. Lighting information from the images is mathematically synthesized to build a mathematical model of the surface, enabling a user to re-light the RTI image interactively and study its surface on a screen (Schroer et al., 2014).

By RTI viewing software, each constituent pixel can reflect the software's interactive “virtual” light from any position this changing interplay of light and shadow in the image discloses fine details of the subject's 3D surface form (Palma et al., 2010).

3.1. Two Types of RTI Were Applied.

3.1.1. RTI VIS.

The source light in RTI VIS is external flash LED light and the photos captured in visible range.

3.1.2. RTI IR.

Mixing between multispectral imaging (IR) and RTI applied and tested. Mixing and matching between these two techniques can add value to the results can get and help to have a different vision of the interpretation for the surface of the object.

3.2. Tools

3.2.1. Camera.

Nikon D810 DSLR (36.3 MP FX, CMOS sensor) for RTI IR (Figure1) and Canon 5D mark III for RTI VIS.

3.2.2. Lenses.

Tokina 35mm f/2.8 AT-X PRO DX Macro Lens for Nikon which used for RTI IR (Figure 2) and A Canon 50 mm f/1:2.8 AF lens was used for RTI VIS photos.

3.2.3. Light Source.

Near IR K- light illuminator LED Wave Length 780 - 1020nm which used as source light for RTI IR (Figure 5) and Canon Speedlite 580EX II Flash as source light for RTI VIS.

3.2.4. Spheres.

Two black spheres were used as targets in the both techniques (Fig 14).

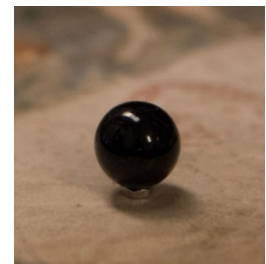


Figure 14. Spheres.

3.2.5. Software.

RTI Builder, RTI Viewer (Figure 15) and CANON EOS Utility 3.

3.3. Procedures of RTI Imaging.

3.3.1. RTI VIS.

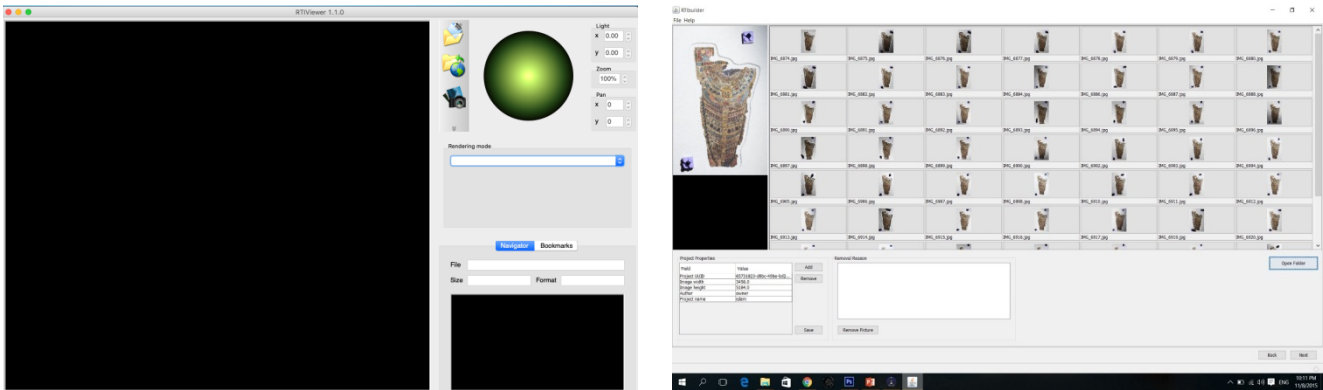


Figure 15. RTI Builder & Viewer Software.

The objects were photographed along with two shiny black spheres and illuminated by a light source Canon Speedlite 580EX II Flash manually held in position using a digital camera Canon 5D mark III DSLR (CMOS sensor) fitted with Canon 50 mm f/1:2.8 AF lens.

The camera was operated in fully manual mode with setting (ISO= 100 -Shutter speed 160 – F Number 11) and was tethered to a computer using live view mode. 45 photos were taken with the same setting but for each photograph, the light is moved to a different position and angle, always maintaining the same distance from the subject which should be 3.5 times the size of the object photographed, thus creating an imaginary dome around it.

Through a set of mathematical calculations made by RTI Builder, the surface normal are identified and consequently, the object's topography and reflective properties. The final file is viewed by RTI Viewer software.

3.3.2. RTI IR.

The objects were photographed along with two shiny black spheres and illuminated by a light source near IR K- light illuminator LED manually held in position using a digital camera Nikon D810 DSLR (CMOS sensor) fitted with Tokina 35mm f/2.8 AT-X PRO DX Macro Lens (Figure 16). The camera was operated in fully manual mode with setting (ISO= 100 -Shutter speed 20 – F Number 11) and was tethered to a computer using live view mode. 45 photos were taken the same angles and technique of moving light like RTI VIS.



Figure 16. RTI setup for RTI IR.

4. X-ray Radiography.

X-ray radiography or computer tomography are standard techniques widely used and accepted. These methods enable information about the manufacturing process and the condition of an object without “touching” the artifacts. That structure and different paint layers can partly be studied by technical means of X-ray radiography, where due to the varying absorption of X-ray radiation, e.g. by the pigments used, a visualization of the material distribution can be achieved. Usually, details and also changes in the design of an object can be shown (Passmore et al., 2012).

X-radiography is useful for the coffin and it's usually used to clearly identify the location of the original metal pins used to fix the items of wooden furniture which is not visible from the surface of the object and this was used in addition too as an evaluation method of construction and wood condition (parkes et al., 2010). Internal areas of loss or weakness within the material are also clearly visible, as are the joins between separate pieces. Modern fill materials used to compensate for areas of loss generally appear different in the X-radiographs as these areas dense are different than the original substrate.

The instrumentation for such investigations is very simple and a plot is given in Beside the X-ray source, the object and an X-ray sensitive material for the detection of the transmitted radiation, e.g. film is required. Coffin box was scanned using a quattro slate 25* 30 cm wireless cesium – I detector system with tablet monitor (Figure. 17).

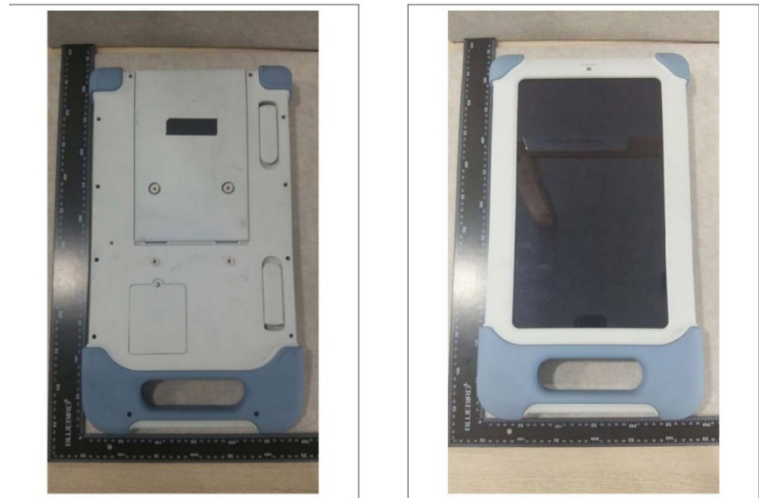


Figure 17. Cuattro Slate Cesium–I Detector System.

Photo source: <https://fccid.io/>

5. X-Ray Fluorescence (XRF) Analysis.

X-ray fluorescence (XRF) spectrometry is a widely used non-destructive technique for the measurements of the elemental composition of materials. XRF is based on the principle that individual atoms when excited by an external energy source, emit X-ray photons of specific energy or wavelength. By counting the number of photons of each energy emitted from a sample, the elements present may be identified and quantitated.

The identification of elements by X-ray methods is achievable due to the characteristic radiation emitted from the inner electronic shells of the atoms under specific conditions. The emitted quanta of radiation are X-ray photons whose specific energies permit the identification of their source atoms (Archaeometry, n.d.).

5.1. Analysis's Devices.

The measurements were performed with a Niton™ XL3t GOLDD handheld XRF spectrophotometer instrument using the NITON XL3t X-ray tube-based analyzer with Ag anode, 50kV, and 0-200μA max (Figure. 18). The instrument head was placed in contact with the selected area and the irradiated area was about a 3mm radius.

All points were exposed for a minimum of 60 seconds using mining mode. XRF spectra were produced using TMNiton Data Transfer (NDT) software. The analysis was performed at the XRF Laboratory at the Conservation Center, Grand Egyptian Museum (GEM-CC). Seven spots were analyzed from the cartonnage object from different points presents different colors and around twelve spots from the coffin from different colors too. This analysis was used as a complementary analysis for the identification of the pigments.



Figure 18. Niton™ XL3t GOLDD hand held XRF spectrophotometer.
photo Source: www.nasional-construction.com

6. Digital Microscope (VHX-950F Series).

The painted layers were observed and analyzed under a Digital Microscope VHX-950F Series (Figure. 19). Images of observed layers was easily recorded on-site using an integrated high-capacity 500 GB HDD, a 1600 (H) × 1200 (V), approx. 1000 TV lines on the computer screen. Pictures have been acquired with the program VHX-950F Application Suite. The VHX-950F microscope enabled a wide range of observation from macro-scale stereoscopic imaging to the detailed analysis of a Scanning Electron Microscope (SEM). Many techniques are supported, including transmitted and polarized lighting, as well as differential interference contrast. The high-speed filing system ensures stress-free handling of a large quantity of images. Lens, magnification, lighting, and measurement data can be saved on the VHX-950F and recalled later. The VHX-950F enables a Wide magnification range from 0.1× to 5000× with a single unit.

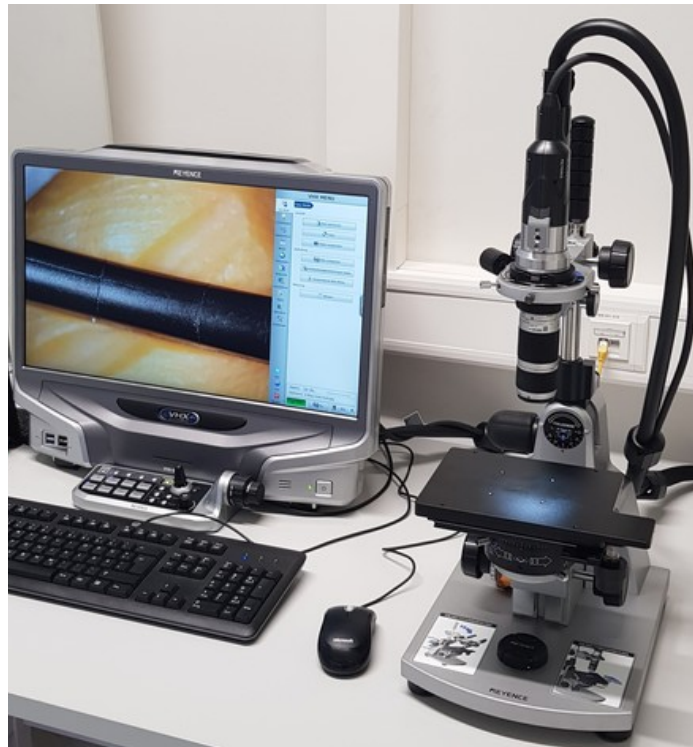


Figure 19. Digital Microscope VHX-950F Series

(Photo: <https://www.ulman.de/>).

#	Methods	Utilization
1	VIS-Visible light	This is the usual color photograph of the painting serving as the reference for the other images.
2	VISTR-Visible Transmitted	The painting is illuminated by visible light and the transmitted light is recorded on the other side of the painting. It allows a better separation of paint layers and can make later alterations more visible.
3	RTI-Reflectance transformation Imaging	Allows the interactive re-lighting of the topic from any direction and the mathematical enhancement of the subject's surface shape and color properties. The enhancement functions of RTI reveal surface information that's not disclosed under direct empirical examination of the object.
4	UVF-Ultraviolet Fluorescence	The painting is illuminated by ultraviolet radiation and the resulting fluorescence is recorded. Varnishes and retouching become visible in this manner.
5	UVR-Ultraviolet Reflected	The painting is illuminated by ultraviolet radiation and the reflected UV radiation is recorded.
6	UVRFC-Ultraviolet Reflected false color	Images created through digital post- processing by combining visible and ultraviolet reflectance (UVR) images. The false colors produced can help in characterizing materials or in distinguishing between visually similar substances.
7	IRR-Infrared Reflectography	The painting is irradiated by infrared radiation and the reflected radiation is recorded. IR-radiation penetrates the surface layers of the painting and the underdrawings becomes visible.
8	IRFC-Infrared False Color	Is created by combining a visible picture and an infrared picture, thus making it possible to observe the different materials and retouches in the false color image.
9	IRF-Infrared Fluorescence.	The painting is illuminated by visible or infrared rays and the resulting fluorescence in the infrared region of the spectrum is recorded. Some pigments such as cadmium yellow fluoresce in the infrared region and can be detected in this manner.
10	IRTR-Infrared Transmitted.	The painting is irradiated by infrared radiation and the transmitted radiation on the other side of the painting is recorded. It gives in some cases a better visual representation of underdrawings and alterations.

Table 1. Summary of the different methods which were used in the Methodology.

Chapter Four: Results

Chapter Contents:

1. Case Study 1: Wooden Coffin Lid (GEM No. 22452).

- **1.1. Ultraviolet Florescence.**
- **1.2. Infrared Florescence.**
- **1.3. Infrared False Color (IRFC).**
- **1.4. Infrared.**
- **1.5. X- Ray Radiography.**
- **1.6. Reflectance Transformation Imaging (RTI).**
- **1.7. X-ray Fluorescence (XRF) Analysis for the Painted Layers.**

2. Case Study 2: Cartonnage Mummy Trappings (GEM No. 8615).

- **2.1. Ultraviolet Fluorescence (UVF).**
- **2.2. Ultraviolet Reflected (UVR).**
- **2.3. Ultraviolet Reflected False Color (UVRFC).**
- **2.4. Infrared IR.**
- **2.5. Infrared Fluorescence IRF.**
- **2.6. Infrared Fluorescence False Color.**
- **2.7. Infrared False Color.**
- **2.8. Visible Transmission.**
- **2.9. IR Transmitted.**
- **2.10. IRFC Transmitted.**
- **2.11. Reflectance Transformation Imaging (VIS RTI – IR RTI).**
- **2.12. X-ray Fluorescence (XRF) Analysis.**

1. Case Study 1: Wooden Coffin Lid (GEM No. 22452).

Corroborating the analytical techniques of imaging and spectroscopy i discuss separately, the different methods were applied and evaluate it according to the effective and the importance. This work illustrates the application of a multispectral system for the examination of art and historical objects of different sizes first the spectral documentation of the wooden coffin as first object is discussed, involving adaptation of the panoramic photographic method. which is very rich in studying so applying the different techniques (Ultraviolet Florescence, infrared Florescence and infrared) (Figure. 20) given the chance to extract information of manufacturing techniques, pigments, preparing layers and the application Sequence.



Figure 20. Coffin full image from left A-Visible – B-UVF – C-IRF – D-IR.

1.1. Ultraviolet Florescence

Through multi spectral imaging techniques by exposing the coffin to the Ultraviolet light – ultraviolet-florescence (UVF) images showed that there is hue in different spots in the body of the coffin which is evidence for the presence of varnishes, while fluorescence of yellow areas suggests that a yellow painted layer probably made of arsenic based pigments since it gave fluorescent properties.

The dark violet places give strong evidence of previous conserve work and shows that this coffin exposed for different treatment processes like using wax and repaint for different colors such as the blue color which is in the mask part and the orange color in the hands and chain which is totally retouched which appear as dark violet under UV (Figure. 21), in addition, some points were observed in the figure areas, such as the scarab, in which the restoration work was done using wax mixed with green color and re-coloring in other areas along the body of the coffin (Figure. 20 B).

The green painted areas didn't show any UV fluorescence (Figure. 20 -21). This could be an indication of the presence of copper- based pigments, since they are known to quench fluorescence of surrounding media. Areas of red pigment appeared darker. This is particularly evident, which may suggest that the red pigment is red ochre (colored by hematite, Fe_2O_3), consistent with the strong quenching properties of iron-based pigments. Black pigments appear darker too and that's clear in some parts like eyes and beards which may suggest that the black pigment is a carbon- based black, consistent with the strong absorption properties of carbon.



Figure 21. UV details of the chest and middle part of the coffin.



Figure 22. UV clear details showing the retouches of previous treatment.

1.2. Infrared Florescence

In the infrared Florescence image (Figure. 20c and 23), the blue color appeared as bright white. The luminescence of such areas could indicate the presence of Egyptian blue. IRF photography allows the mapping and detection of Egyptian blue.

In the mask part (Figure. 23), we find that there is a difference in the blue color, where the upper part appears in white, which, as we mentioned beginning, is likely to be the Egyptian blue, as for the rest of the blue parts, which appear dark, this indicates the difference in the color material, which confirms the theory of previous restoration procedures and touches Which was done on parts of some figures (Figure. 24) in the coffin which detected too by UVF.



Figure 23. Details of IRF showing different in blue color.

IRF images (Figure. 20c and 23) didn't show any luminescence of the green painted areas, therefore the hypothesis of a mixture of Egyptian blue and yellow pigments can be discarded but still there is probability of using this Mixture in Dark green.



Figure 24. Clear details.

1.3. Infrared False Color (IRFC)

Infrared false color image (Figure. 25 and 26) indicated that the areas painted with blue pigment appeared red, which confirm the presence of Egyptian blue which was detected too in IRF. Infrared false color images (Figure. 26) show that the painted green areas appear with a lighter blue hue, which suggests the use of malachite. Carbon-based black is one of the pigments which has indication too in the infrared false color image where the black appeared black and that is detected in the eyes points.

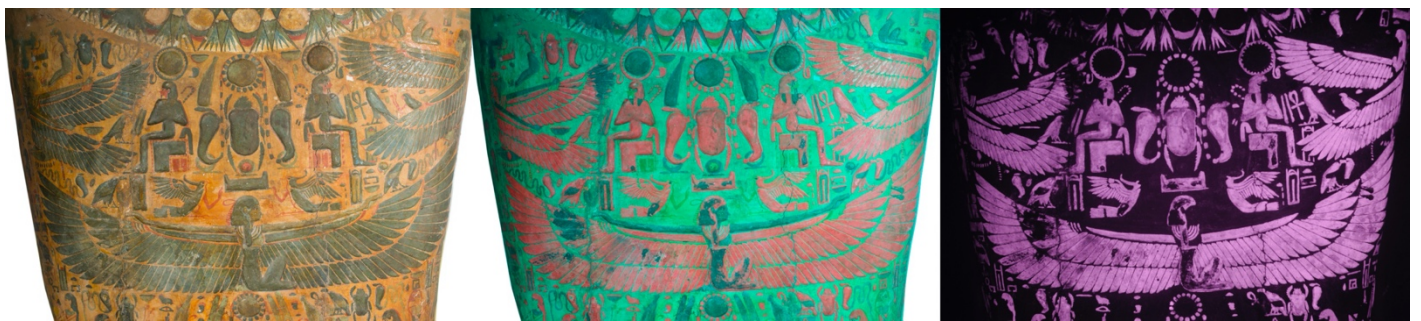


Figure 25. Left: visible and IRFC in the middle – on the right IR.



Figure 26. Details IRFC.

1.4. Infrared

In the IR image (Figure.27) the base red lines are not clear but IR image suggested the presence of carbon based black pigment, which is opaque under IR. Also IR image revealed the black outlines, which did not clearly appear in the visible. Hidden black outlines was difficult to see it under the blue and green painted layer. This is due to carbon black or copper-bearing pigments such as Egyptian blue are opaque under infrared emission and appear dark.



Figure 27. Details of IR.

1.5. X- Ray Radiography

The use of X-ray gave a complete idea of the shape of the coffin and the locations of the wooden connections used, which appeared in some points and to be absent in some places. The appearance of light places in some areas, such as the ear and the wig, proves the truth of using a coarse paste, which was applied in some places with the coffin to smooth out major irregularities.

Also, the ornamental figures represented by the scarab and the sun, which appeared clearly in a different degree of contrast, which was most likely made of paste too and was then applied to the coffin and then different colors were applied to it.

At to that X-ray radiograph showing details of the deterioration aspects not visible to the naked eye, e.g. longitudinal cracks and gaps under the painted gesso layer.



Figure 28. X-Ray radiography.

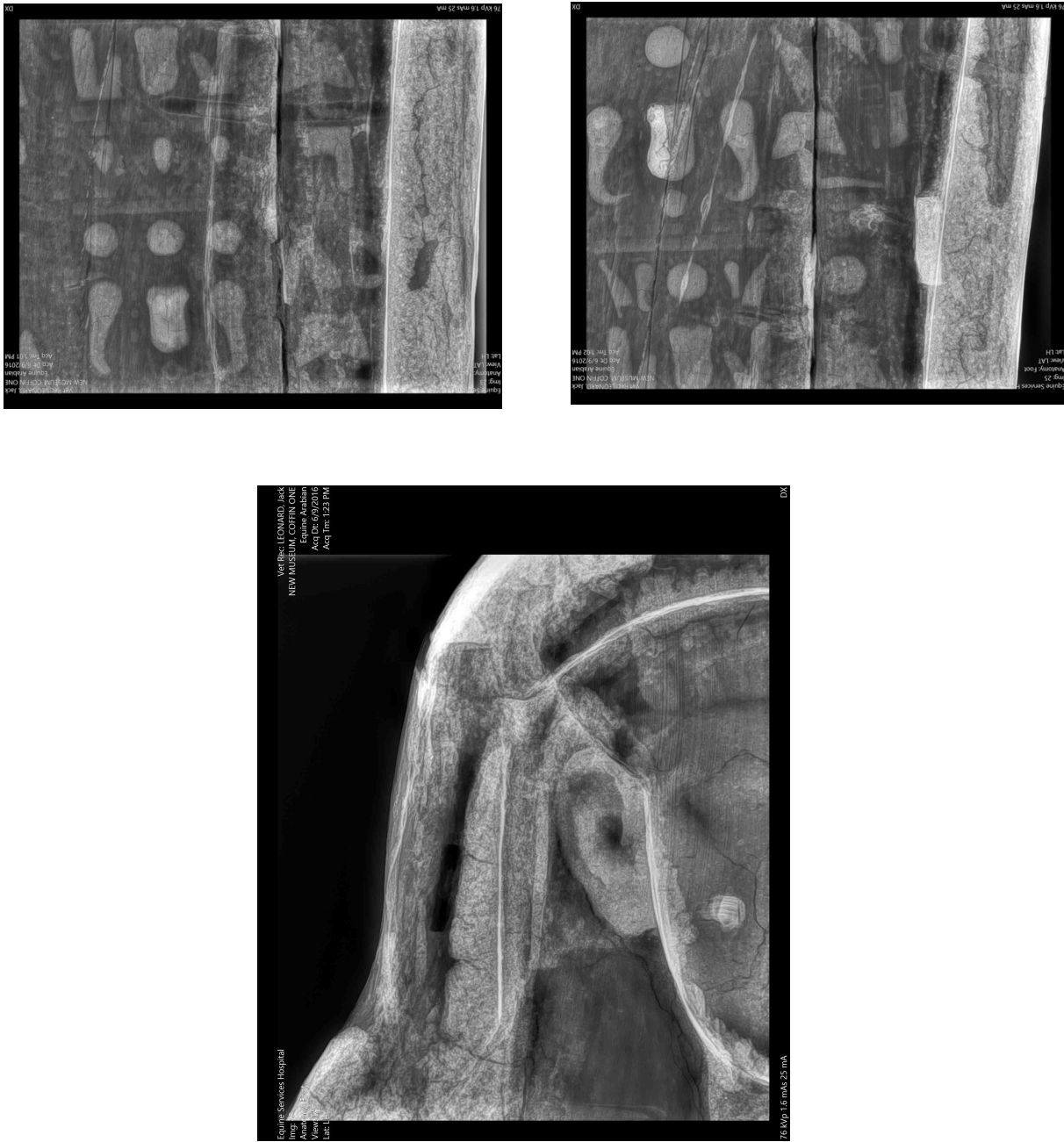


Figure 29. Details showing ornamental figures represented by the scarab and the sun (Up) and the ear which appears in coarse paste (Down).

1.6. Reflectance Transformation Imaging (RTI)

Sometimes finger prints are used in varnish layers, that's make us very near to the people who handled the coffins in ancient times. As the fact that hands are probably the most tools of any craft, there is very little evidence for the use of hands for the application of paint or the application of preparation layers on coffins or other ancient Egyptian objects but in this case no evidence were detected on the surface of the coffin.

By using RTI and analyse the photos by changing between different filters of RTI viewer program Broad brushstrokes in the ground layers are visible and detected in many points of the coffins (Figure 30 B), indicating that the white under-layers have not been burnished before applying the colored decoration. The brush strokes are about 4 cm wide and follow scattered mainly in half circular patterns, just like anybody today would apply a paint coat.

The brushstrokes are clearly visible in specular mode (Figure 30 c) because of the use of relatively coarse pigments and a water-based binding medium (mainly gum Arabic). A paint with this combination of materials is not able to form a smooth film with drying, and therefore the brush strokes remain visible. Finer lines were detected clearly by normal visualization filter in some shapes that's because of tools which used to apply the red and blue sections of the polychrome probably fine brushes and Hollow pens were used (Figure. 30 D). Specular filter shows the grainy surface of the yellow painted layer and shows also inhomogeneous in thickness (Figure 31). After examining through the RTI, it became apparent that these black lines (Figure 32) were most likely modern lines during the period in which the coffins were restored, as they appear clearly in the RTI image that it was applied above the original colors on the coffin.

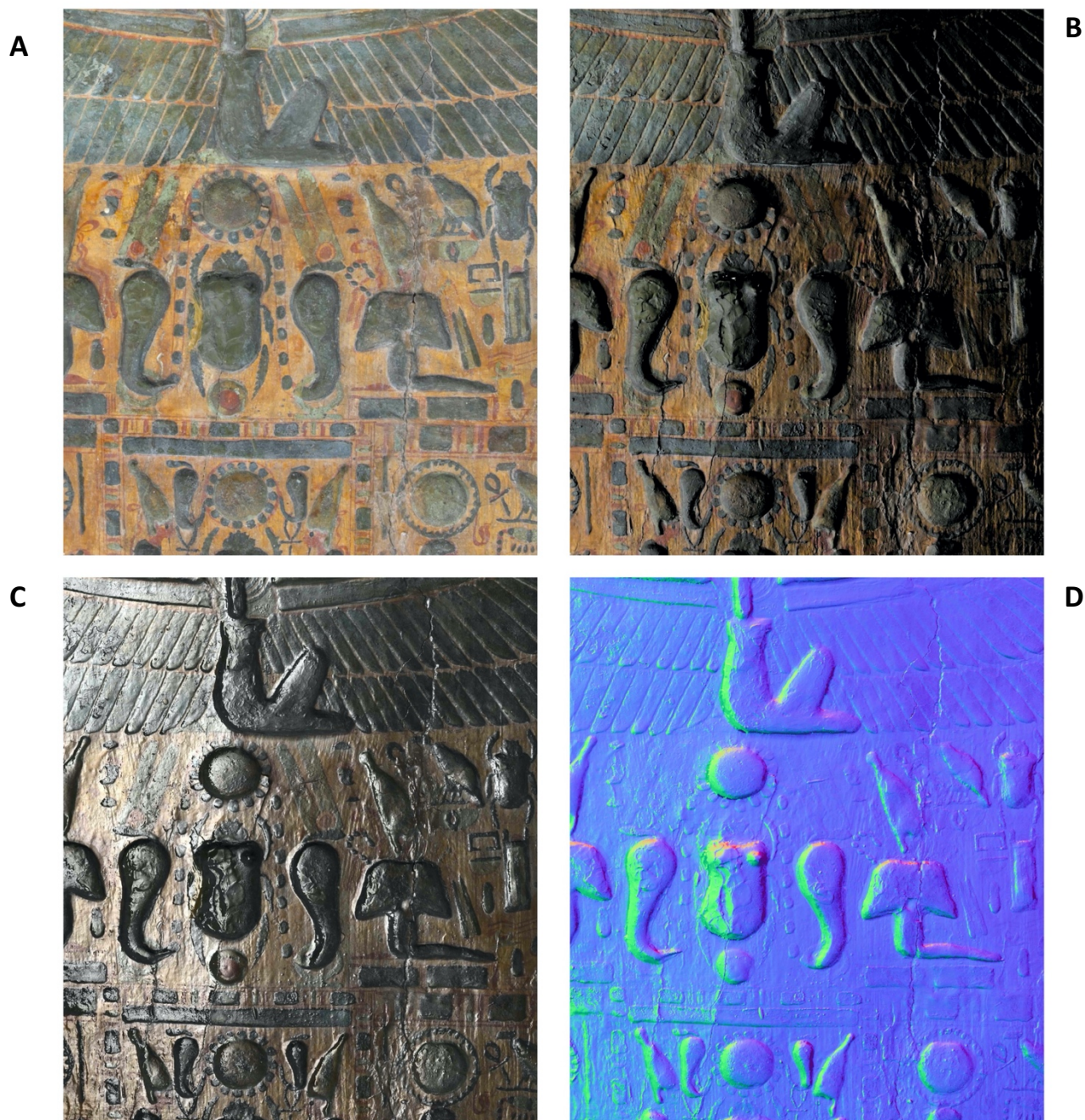


Figure 30. RTI Details of Coffin. A – Visible B- Diffuse gain C- Specular enhancement D- Normal visualization.



Figure 31. Details of the grainy surface of the yellow painted layer.

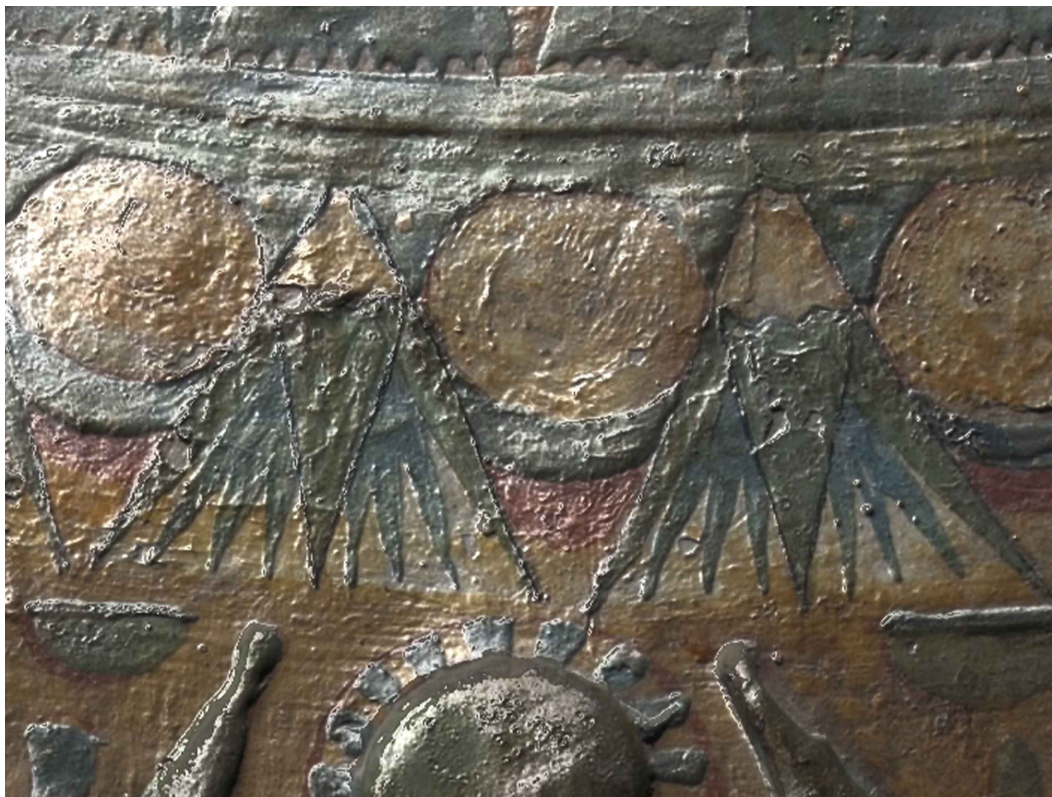


Figure 32. Details of black lines.

1.7. X-ray Fluorescence (XRF) Analysis for the Painted Layers

Portable X-ray Fluorescence spectrometry (pXRF) is a method for locating heavy elements on a painted surface, using a portable device. This is a quick and non-invasive method that helps with starting to identify inorganic pigments.

A XRF study of wooden coffin lid painting provided significant information about the pigment composition. This information about the pigment composition revealed the presence of different type of pigments were used.

All the XRF spectra, acquired on the surface of the polychrome anthropoid wooden coffin and Cartonnage mummy trappings, showed the peaks of calcium and silicon, related to the calcite and quartz in the preparation layer.

1.7.1. Yellow Painted Layer

The result of XRF analysis (Table. 2) showed presence of calcium (Ca), iron (Fe), sulphur (S), Alumina (Al) and silicon (Si) with traces of arsenic (As) and potassium (K). This result provides evidence for the presence of two yellow colorants arsenic sulphides based pigment that is possibly orpiment As_2S_3 and yellow ochre Iron oxyhydroxide $FeO(OH)$.

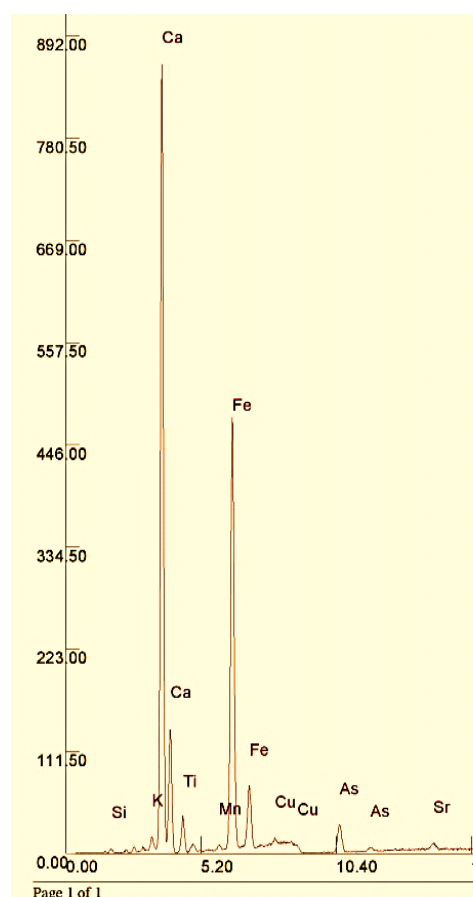


Chart 1. Yellow pigment chart.

Chapter Four: (Results)

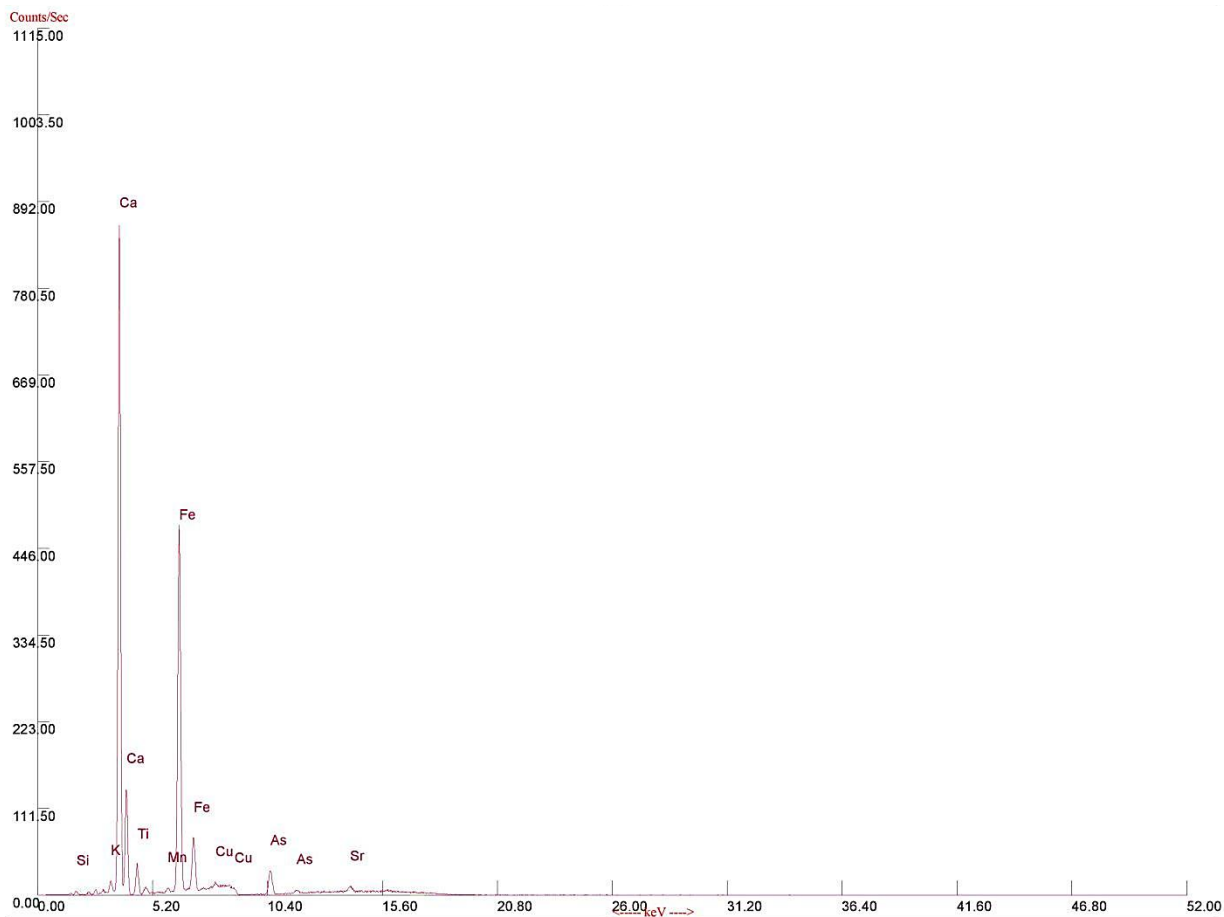


Chart 2. Chart of yellow pigment.

Composition of Yellow Color						
Elements	Area 1		Area 2		Area 3	
	%	Error	%	Error	%	Error
As	0.179	0.008	0.414	0.012	0.206	0.008
Zn	0.005	0.003			0.006	0.003
Cu	0.013	0.004	6.660	0.110	0.023	0.005
Fe	2.014	0.071	1.260	0.040	1.794	0.065
Mn	0.040	0.023				
Cr	0.015	0.007				
Ti	0.331	0.030	0.056	0.019	0.322	0.031
Ca	18.244	0.372	8.022	0.228	20.326	0.380
K	0.466	0.047	0.408	0.041	0.603	0.049
Al	2.055	0.313			1.053	0.378
P	0.260	0.067			0.202	0.099
Si	7.404	0.278	2.486	0.385	5.375	0.361
Cl	0.737	0.026	1.403	0.074	0.998	0.044

S	1.934	0.076	1.593	0.150	2.161	0.118
Zr	0.016	0.001	0.017	0.001	0.022	0.001
Sr	0.052	0.002	0.054	0.002	0.052	0.002
Pb			0.016	0.002		

Table 2. The results of X-ray fluorescence (XRF) for the yellow color.

Composition of Yellow Color								
Elements	Area 4		Area 5		Area 6		Area 7	
	%	Error	%	Error	%	Error	%	Error
As	1.845	0.041	0.048	0.004	2.280	0.055	1.554	0.029
Zn	0.021	0.005	0.094	0.007			0.024	0.003
Cu	0.021	0.005	0.006	0.003	0.007	0.004	0.012	0.003
Fe	0.353	0.029	1.838	0.066	0.157	0.023	0.667	0.031
Mn	0.048	0.022	0.040	0.023			0.080	0.019
Cr	0.009	0.006	0.017	0.010			0.025	0.011
Ti	0.073	0.018	1.883	0.081	0.032	0.014	0.444	0.083
Ca	17.359	0.359	19.925	0.381	10.801	0.320	18.715	0.367
K	0.809	0.055	0.406	0.046	0.111	0.036	0.156	0.040
Al	0.714	0.262	1.115	0.306			0.691	0.214
P								
Si	3.361	0.221	4.918	0.274	0.802	0.139	2.046	0.161
Cl	1.147	0.037	1.002	0.036	0.473	0.026	0.636	0.024
S	5.988	0.148	3.894	0.124	2.744	0.110	3.193	0.094
Zr	0.017	0.001	0.017	0.001	0.021	0.002	0.007	0.001
Sr	0.062	0.002	0.092	0.003	0.041	0.002	0.068	0.002
Pb			0.004	0.002			0.003	0.001
Mg	3.444	1.571			2.509	1.260		

Table 3. The results of X-ray fluorescence (XRF) for the yellow color.

1.7.2. Blue Painted Layer

According to XRF spectrum of the blue painted layer (Table 4), the elements that presented the highest concentrations were silicon (Si), copper (Cu), and Calcium (Ca). This result provides evidence for the presence of copper -based pigment that is most likely Egyptian blue Calcium copper silicate ($\text{CaCuSi}_4\text{O}_{10}$).

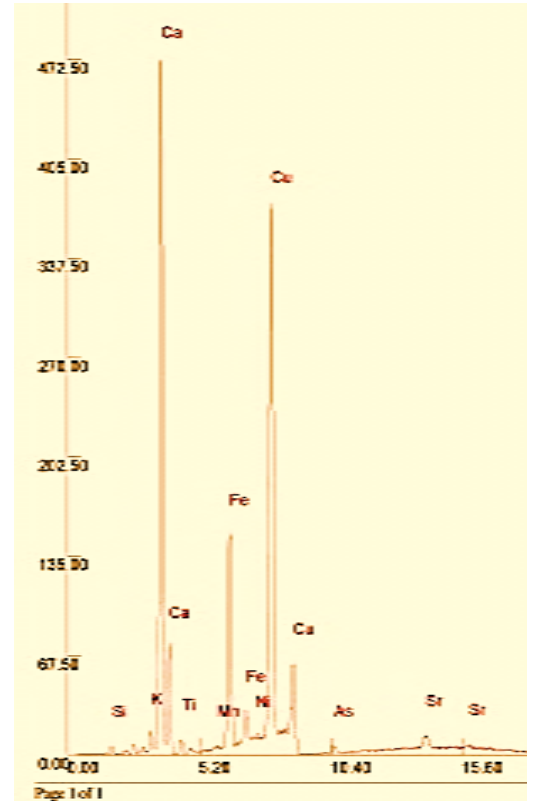


Chart 3. Blue pigment chart.

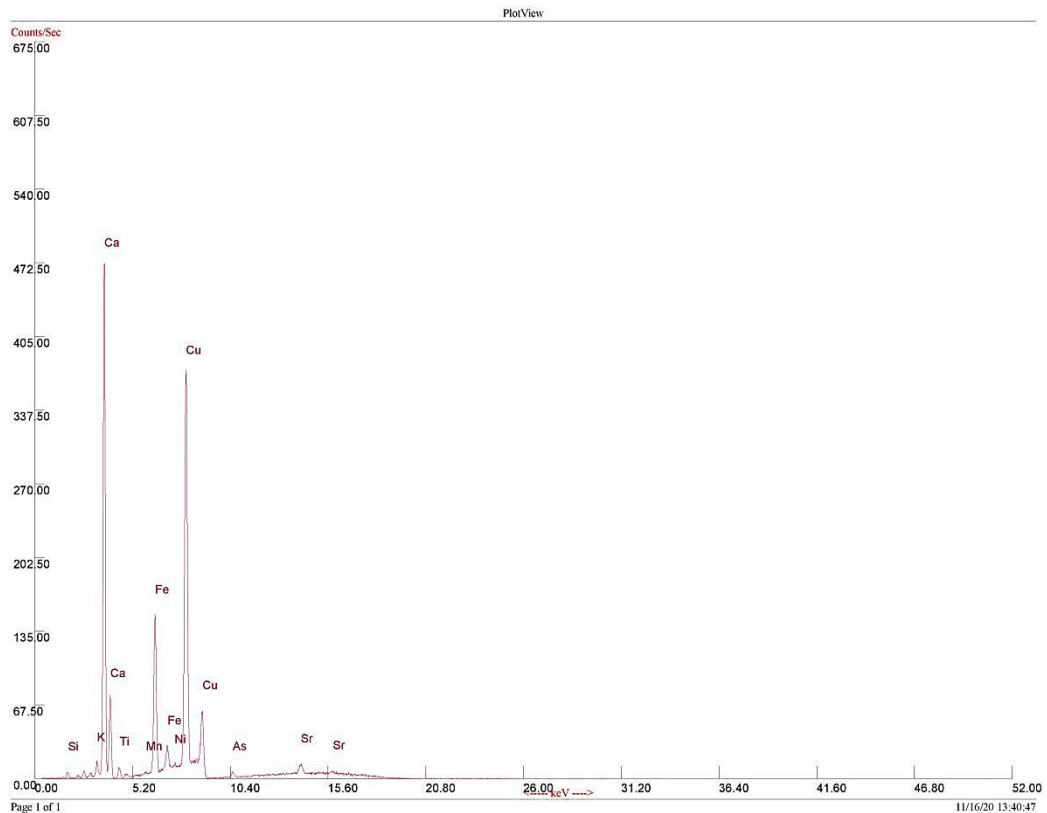


Chart 4. Chart of Blue pigment.

Composition of Blue Color						
Elements	Area 1		Area 2		Area 3	
	%	Error	%	Error	%	Error
Sr	0.060	0.002	0.011	0.001	0.074	0.003
As	0.031	0.003	0.024	0.003	0.023	0.003
Pb	0.010	0.002	0.007	0.002	0.006	0.002
Cu	5.369	0.105	3.464	0.073	0.954	0.032
Fe	0.378	0.026	0.586	0.034	0.411	0.033
Ti	0.043	0.016	0.068	0.017	0.278	0.098
Ca	13.625	0.321	10.905	0.277	17.287	0.390
K	0.339	0.043	0.432	0.044	0.162	0.041
Al	0.757	0.253	0.408	0.184	0.626	0.320
Si	10.374	0.353	10.247	0.319	2.418	0.276
Cl	0.887	0.032	0.888	0.029	0.476	0.033
S	2.373	0.093	1.553	0.068	3.922	0.163
Sr			0.068	0.002		
P			0.105	0.062		
Mn					0.101	0.029
Cr					0.023	0.013

Table 4. The results of X-ray fluorescence (XRF) for the blue color.

1.7.3. Green Painted Layer

From XRF analysis, (spots 2, 3, 4, 5, 6, 7) the elements that presented the highest concentrations for some spots on the green painted layer were calcium (Ca) and copper (Cu). This result provides the possibility for the presence of malachite basic copper (II) carbonate $2\text{CuCO}_3 \cdot \text{Cu}(\text{OH})_2$.

Chapter Four: (Results)

The result of XRF analysis (areas 1,8,9) shows the presence of silicon (Si), copper (Cu), and Calcium (Ca), with significant amount of iron (Fe) and chlorine (Cl). This result provides evidence for the presence of Egyptian blue and yellow ochre pigment. The presence of chlorine (Cl) could probably point to the presence of halite which may be related to the burial soil that surrounded the object.

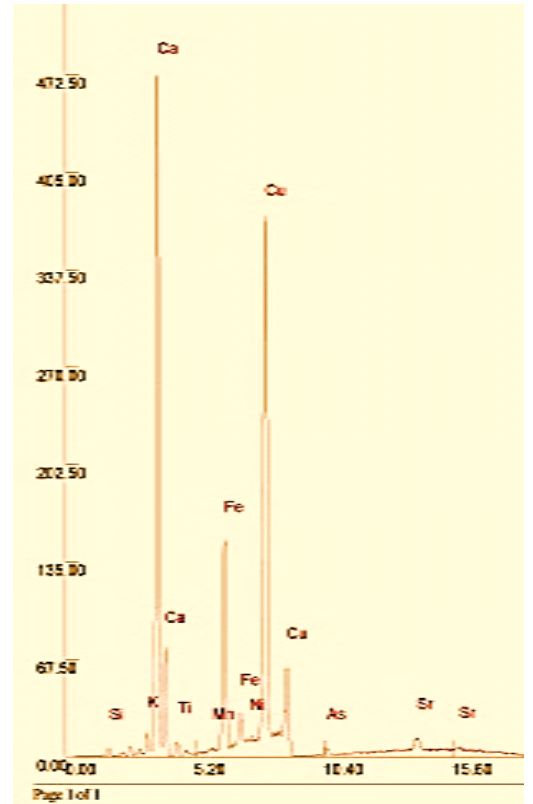


Chart 5. Green pigment chart.

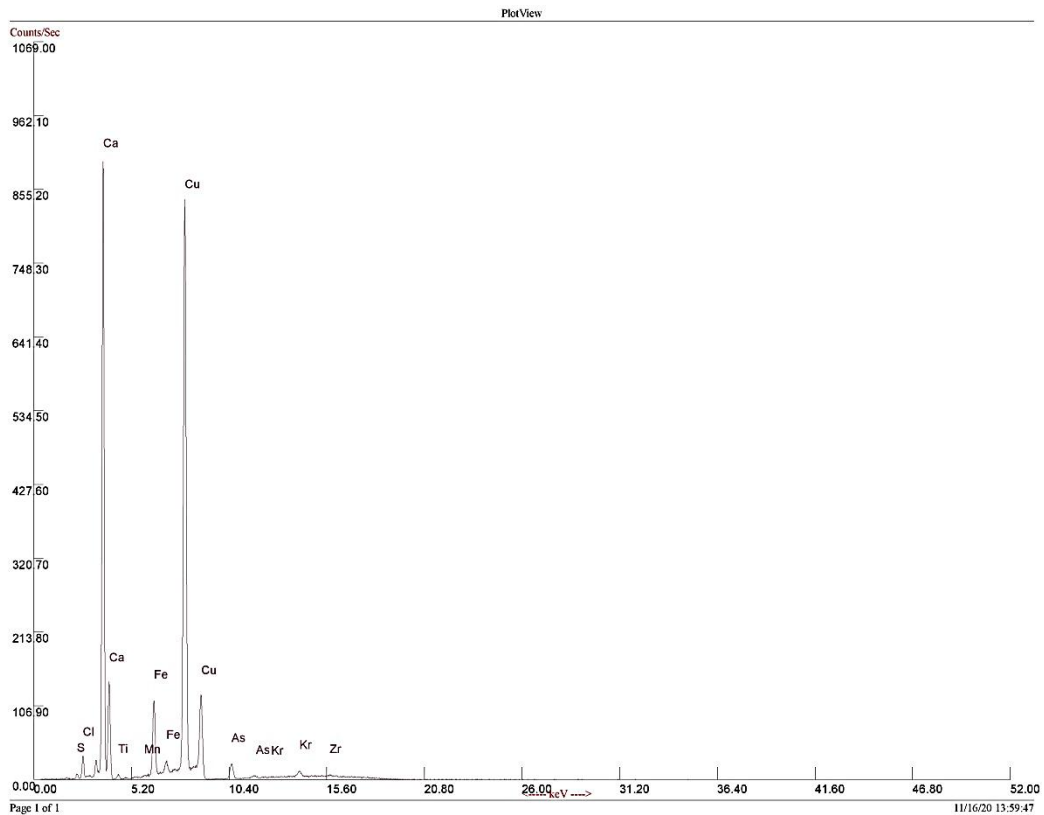


Chart 6. Chart of Green pigment.

Composition of Green Color								
Elements	Area 1		Area 2		Area 3		Area 4	
	%	Error	%	Error	%	Error	%	Error
Sr	0.008	0.001	0.059	0.002	0.033	0.002	0.052	0.002
Cu	0.013	0.002	6.412	0.120	8.083	0.140	5.925	0.114
Fe	2.814	0.048	0.341	0.024	0.428	0.025	0.639	0.034
Ti	0.105	0.025	0.045	0.014	0.039	0.011	0.042	0.013
Ca	3.182	0.117	15.616	0.318	8.048	0.226	8.455	0.241
K	0.048	0.017	0.601	0.048	0.451	0.040	0.595	0.048
Al	0.352	0.140	0.370	0.190	0.765	0.229	0.317	0.194
Si	1.590	0.162	2.954	0.173	14.512	0.377	3.670	0.237
Cl	0.331	0.019	2.413	0.049	0.452	0.021	0.988	0.035
S	2.300	0.088	2.263	0.076	1.422	0.066	1.737	0.082
Sn			0.018	0.007				
As			0.118	0.006	0.044	0.004	0.042	0.004
Pb			0.015	0.002	0.020	0.003	0.016	0.003
P					0.105	0.066		

Table 5. The results of X-ray fluorescence (XRF) for the Green color.

Composition of Green Color								
Elements	Area 5		Area 6		Area 7		Area 8	
	%	Error	%	Error	%	Error	%	Error
Sr	0.046	0.002	0.058	0.002	0.062	0.002	0.124	0.004
Cu	7.800	0.146	10.803	0.195	6.750	0.123	0.023	0.005
Fe	0.321	0.024	0.412	0.025	0.331	0.024	2.104	0.072
Ti	0.035	0.012	0.050	0.013	0.042	0.012	0.634	0.109
Ca	10.536	0.268	8.940	0.251	10.325	0.265	19.945	0.387
K	0.444	0.044	0.576	0.049	0.362	0.041	0.118	0.036
Al			0.708	0.256	0.362	0.217	0.998	0.408
Si	2.182	0.240	3.401	0.222	2.961	0.209	2.093	0.272
Cl	2.605	0.072	2.237	0.054	3.259	0.068	0.535	0.036
S	2.277	0.117	2.074	0.088	1.939	0.086	5.763	0.196
Sn			0.022	0.009	0.012	0.007		
As	0.101	0.006	0.067	0.006	0.095	0.006	0.006	0.002
Pb	0.020	0.003	0.032	0.004	0.014	0.002	0.008	0.002
P			0.107	0.069				
Sn			0.022	0.022				
Mn							0.155	0.031

Table 6. The results of X-ray fluorescence (XRF) for the Green color.

Composition of Green Color		
Elements	Area 9	
	%	Error
Sr	0.052	0.002
Cu	0.030	0.005
Fe	2.499	0.071
Cr	0.012	0.006
Ti	0.107	0.017
Ca	15.170	0.305
K	0.259	0.036
Si	1.604	0.335
Cl	1.320	0.075
S	1.085	0.132
As	0.088	0.005

Table 7. The results of X-ray fluorescence (XRF) for the Green color.

1.7.4. Red Painted Layer

The result of XRF analysis (Table 8) suggest that the red pigment is red ochre Anhydrous iron (III)-oxide (colored by hematite, Fe_2O_3), consistent with the strong quenching properties of iron-based pigments. The results of XRF analysis for some points on the red painted layer showed presence of calcium (Ca), iron (Fe) and silicon (Si) with a high intensity, in addition to a small amount of sulphur (S), copper (Cu) and arsenic (As). This result provides strong evidence for the presence of an iron-based pigment that is most likely hematite Fe_2O_3 .

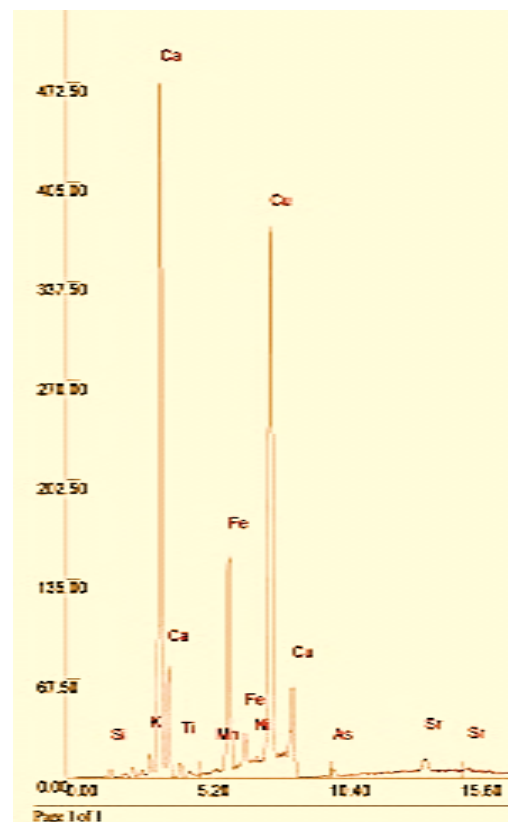


Chart 7. Red pigment chart.

Chapter Four: (Results)

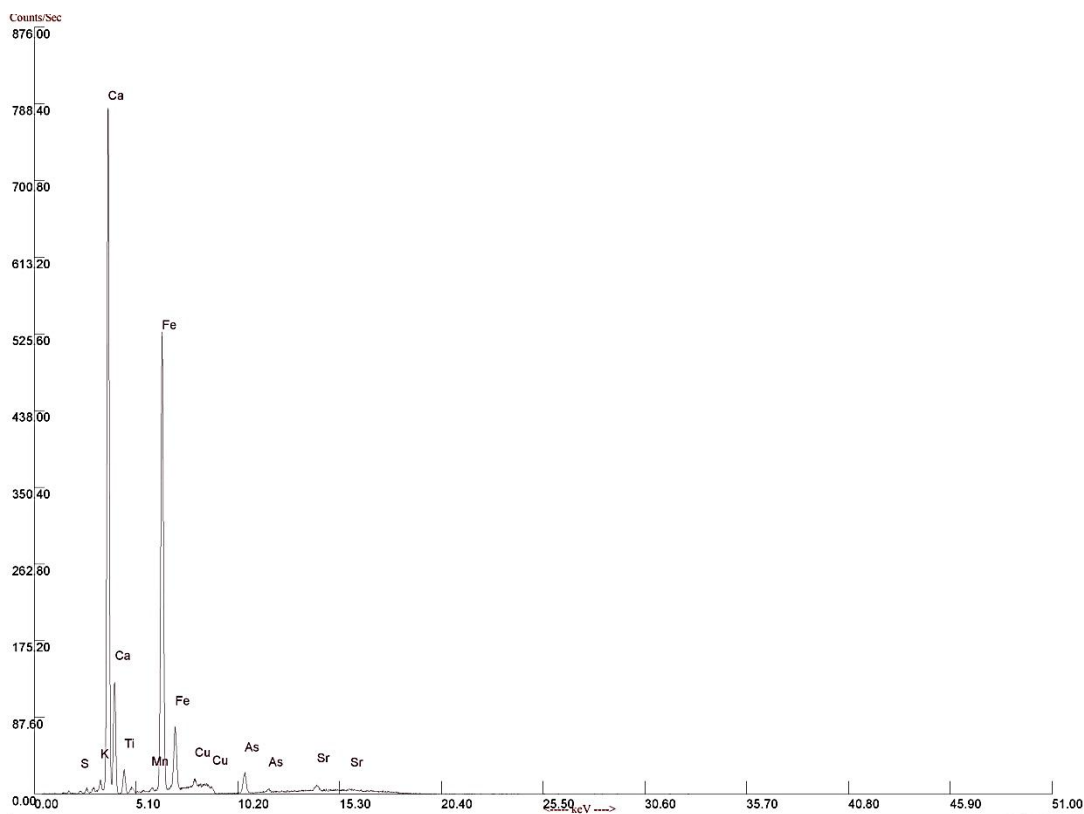


Chart 8. Chart of Red pigment.

Composition of Red Color								
Elements	Area 1		Area 2		Area 3		Area 4	
	%	Error	%	Error	%	Error	%	Error
Sr	0.052	0.002	0.044	0.002	0.443	0.011	0.048	0.002
Zn			0.004	0.002	0.019	0.004		
Cu	0.065	0.008	0.030	0.005	0.028	0.005	0.067	0.007
Fe	2.201	0.081	1.093	0.051	1.148	0.053	2.907	0.084
Cr	0.015	0.008			0.031	0.014	0.015	0.006
Ti	0.268	0.031			0.478	0.110	0.118	0.019
Ca	19.543	0.413	27.174	0.450	28.583	0.495	16.522	0.347
K	0.402	0.048	0.290	0.040	0.120	0.039	0.247	0.039

Al	1.242	0.328			1.124	0.290	0.451	0.285
Si	5.261	0.300	1.221	0.123	2.983	0.196	2.612	0.272
Cl	0.750	0.033	0.607	0.022	0.600	0.024	1.117	0.047
S	1.825	0.092	0.719	0.045	4.552	0.119	1.373	0.097
As	0.143	0.007	0.027	0.003	0.005	0.002	0.096	0.005
Pb					0.004	0.002		
Mn					0.093	0.028		

Table 8. The results of X-ray fluorescence (XRF) for the Red color.

1.7.5. Black

The result of XRF analysis suggest that the black pigment is made from organic materials which not able to detect by the instrument.

2. Case Study 2: Cartonnage Mummy Trappings (GEM No. 8615)

Through multispectral imaging techniques and reflectance transformation imaging, and the application of available and possible methods, include combining of two techniques to achieve the maximum benefit from examining the pieces and obtaining the largest amount of information. The two combined technique applied to a cartonnage object rich in colors and small in size, which helped in the possibility of applying the methods smoothly and obtaining high-quality results, which I can through it to do the judgment and evaluation of the effectiveness of these methods in studying and examining artifacts. Below I review the methods that were applied and the information that could be obtained.

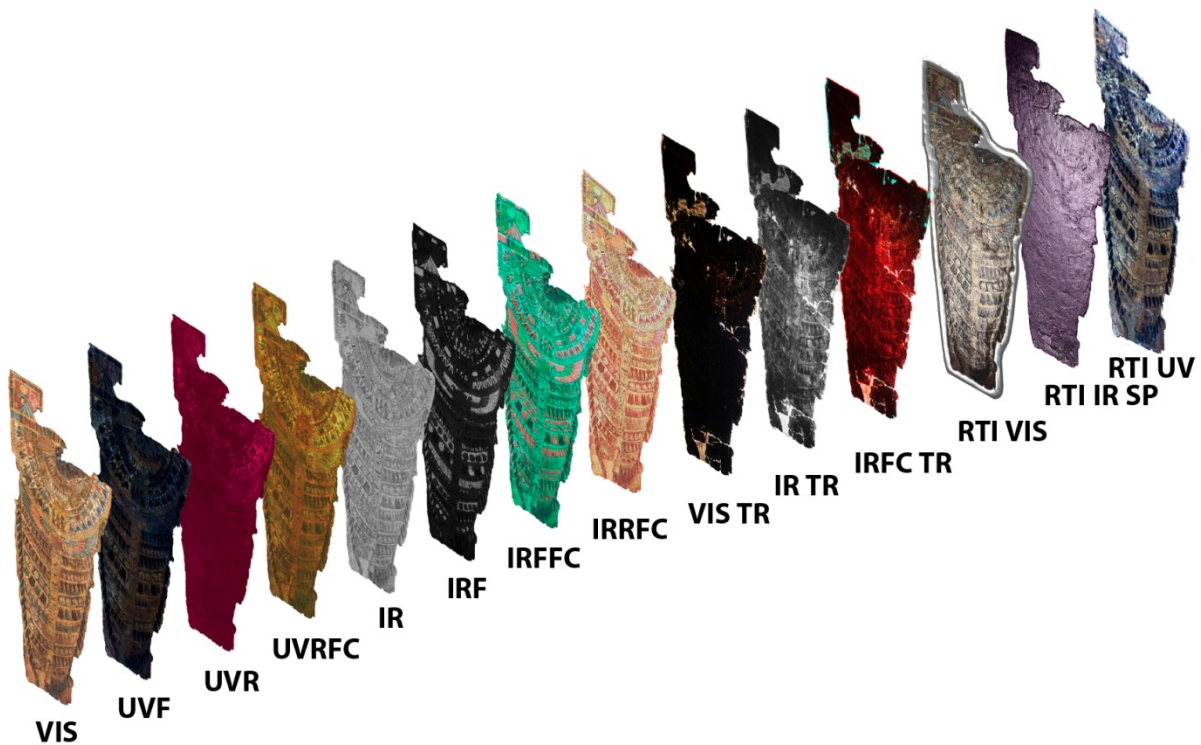


Figure 33. Different methods of MSI were applied.

2.1. Ultraviolet Fluorescence (UVF)

Through multispectral imaging techniques, the object exposed to the Ultraviolet light – ultraviolet-fluorescence (UVF) images showed that there is darkness in different areas and some colors space darker than the others (Figure. 34). Ultraviolet-fluorescence (UVF) images showed also that there is hue in different dots and fibers (Figure. 36) on the surface of the cartonnage which is an evidence for different remains of materials which not belong to the object; it is likely a modern material used the conservation of the object (Figure. 35).

The green painted areas didn't show any UV fluorescence (Figure 34). This could be an indication of the presence of copper-based pigments since they are known to quench the fluorescence of surrounding media. Areas of red pigment appeared darker. This is particularly evident, which may suggest that the red pigment is red ochre (colored by hematite, Fe_2O_3), consistent with the strong quenching properties of iron-based pigments.



Figure 34. UV Fluorescence.



Figure 36. Details of UVF.

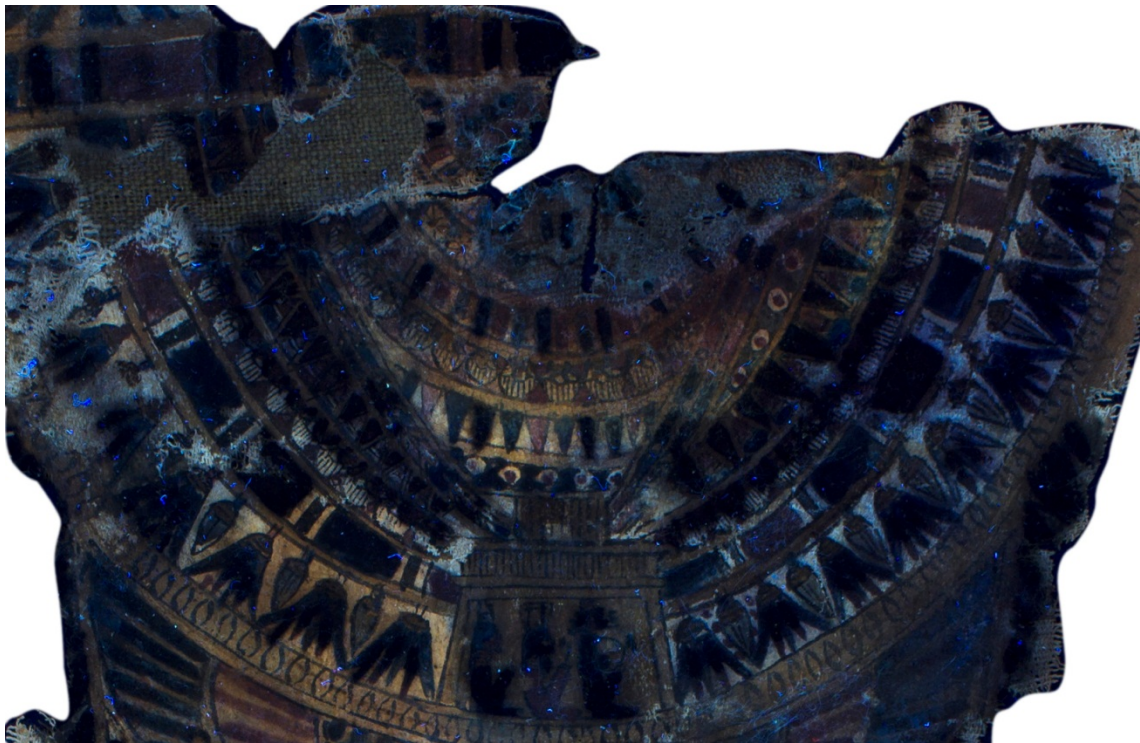


Figure 35. Details of UVF.

2.2. Ultraviolet Reflected (UVR)

UV light interacts just with the very surface layer of paint, so the UVR image is specific to the top most pigment and layers of paint underneath do not influence it. Furthermore, a uniform varnish coating doesn't interfere with the pigments' appearance in the UVR but it will absorb some UV causing just a change in the overall brightness.

Two categories are defined based on the strong differences in the brightness of UV reflected images: first bright and second dark. In UVR photo brightness areas were detected in the top right and top left in some points and this is indicator for the white color it is gypsum which were used for the preparation layer before applying the colors (Figure. 37).



Figure 37. from left: Visible light photo – UVR photo – UVRFC photo.

2.3. Ultraviolet Reflected False Color (UVRFC)

By mixing the channels of visible and UVR images in Photoshop and obtaining a new false color photo from the ultraviolet reflected UVRFC.

Some points were monitored in different colors, the red color appears dark, indicating that probably that the red ocher was used as the red color, and also it was observed that the yellow color appeared in a purple color this is an indication that the yellow color used may be yellow ocher. Moving on to the black lines used in the decorations, they still appear black in the UVRFC which indicator that this black is carbon black (fig 37).

2.4. Infrared IR

In the IR image (Figure. 38), hidden black outlines below the over- red painted layers appeared, while it was difficult in some points to see the black outlines under the blue and green painted layer where the layer is thick and with high intensity. This is due to carbon black or copper-bearing pigments such as Egyptian blue are opaque under infrared emission and appear dark.

Black lines can be clearly seen in most parts of the cartonnage, and it can be noticed that some decorative lines are not drawn or drawn, but they are imprecise and thus lack symmetry, and this may be evidence that the lines are not of great perfection.



Figure 38. Infrared photo.

2.5. Infrared Fluorescence IRF

In the infrared fluorescence image, the blue color appeared as bright white. The luminescence of such areas could indicate the presence of Egyptian blue. Looking at the upper right side of the cartonnage, where there is an intensity of the blue color through the infrared rays, noticed a spreading of blue pigments grains in the surrounding area, which is clearly visible through the bright spots that reveal the Egyptian blue (Figure. 39).

IRF images didn't show any luminescence of the green painted areas, therefore the hypothesis of a mixture of Egyptian blue and yellow pigments can be discarded. However, some dots have been spotted next to the dark green color and it is possible that there is an underlay of Egyptian blue or it is just a decorative drop of Egyptian blue.

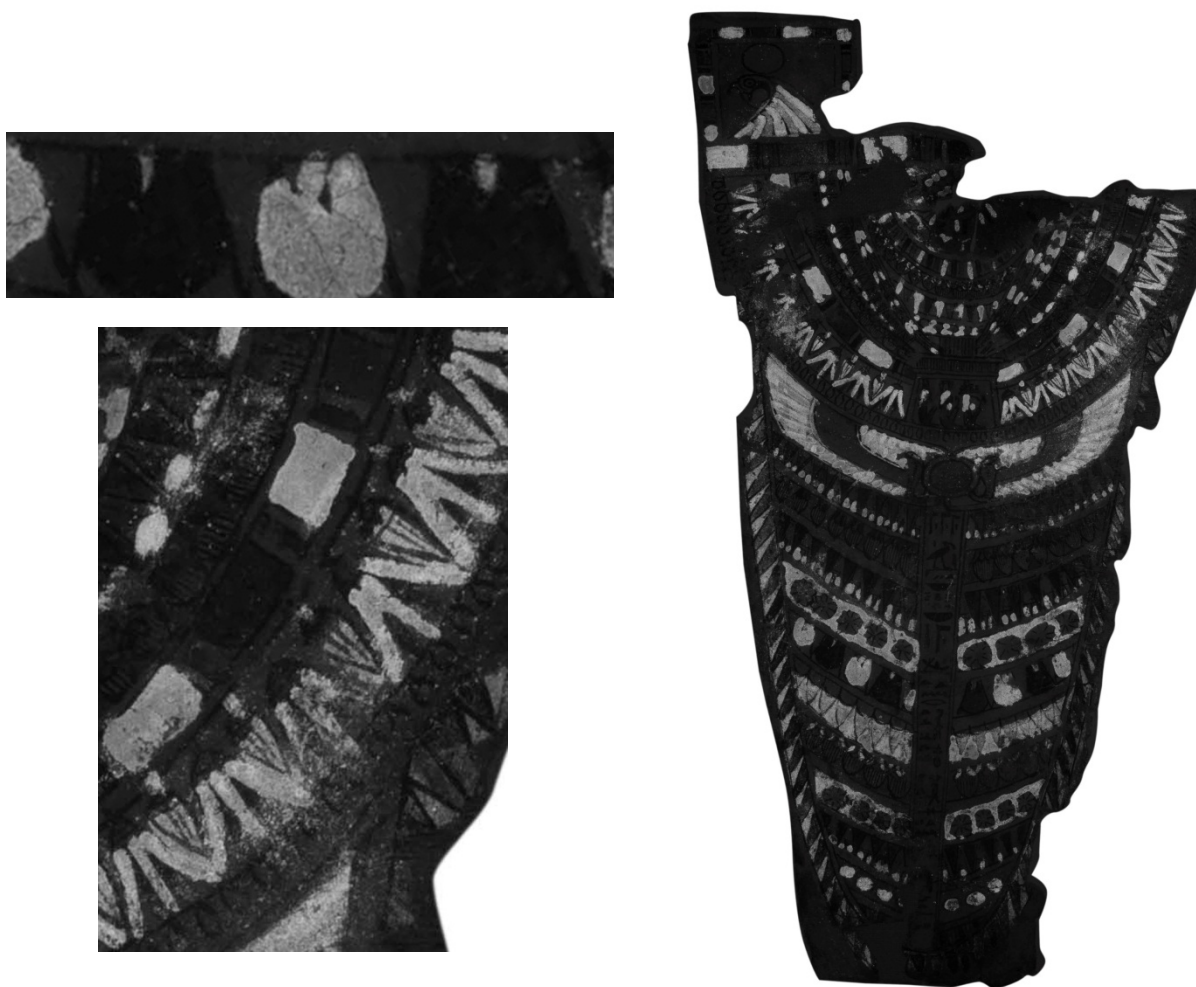


Figure 39. IRF details shows the Egyptian blue.

2.6. Infrared Fluorescence False Color (IRFFC)

Infrared false color image indicated that the areas painted with blue pigment appeared red, which confirm the presence of Egyptian blue. This is a confirmation of what was reached and concluded through the IRF as well (Figure. 40).

2.7. Infrared False Color(IRFC)

Infrared false-color images show that the painted green areas appear with a light blue hue, which suggests the use of malachite which is used in different parts of the painting. In addition to that, some points were monitored in different colors, the red color appears golden yellow, indicating that probably that the red ochre was used as the red color, and also it was observed that the yellow color appeared in a greenish-yellow color this is an indication that the yellow color used may be yellow ochre. Moving on to the black lines used in the decorations characteristically remains dark in false-color images. This is particularly evident in the IRFFC images (Figure. 40).

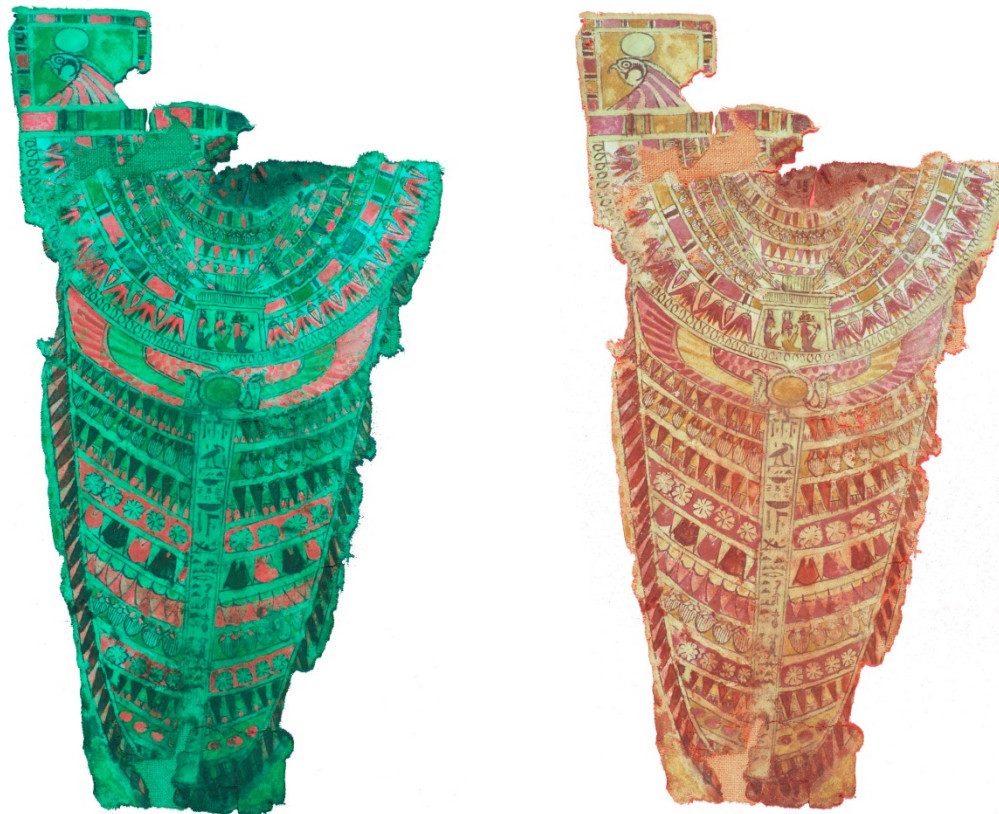


Figure 40. Infrared Fluorescence false color - Infrared false color.



Figure 41. Details shows the yellow, Red and green pigments in the IRFC.

2.8. Visible Transmission

The visible image did not provide much information, but it showed some areas, of which a layer of colors is missing, and others are completely missing both layers of texture and colors, but it did not present much in the areas with full layers.

2.9. IR Transmitted

Infrared Transmittance Imaging was proved to be more suitable and effective for observation of deteriorated aspects of the cartonnage (cracks and fragile parts), and give a mapping for the weakness parts and showed a big difference in the thickness of the regions in all parts of the cartonnage, there are parts that are clear that they have little thickness compared to other parts, and this is clearly visible in pigments such as Egyptian Blue because IR is partially absorbed by materials in the painting.

2.10. IRFC Transmitted

Through Infrared false color transmitted image, I can check the positions and nature of cracks and the information from this image could make sure to supply necessary information to make a plan actual remedial conservation, especially intervention treatment for reinforcement of deteriorated parts.

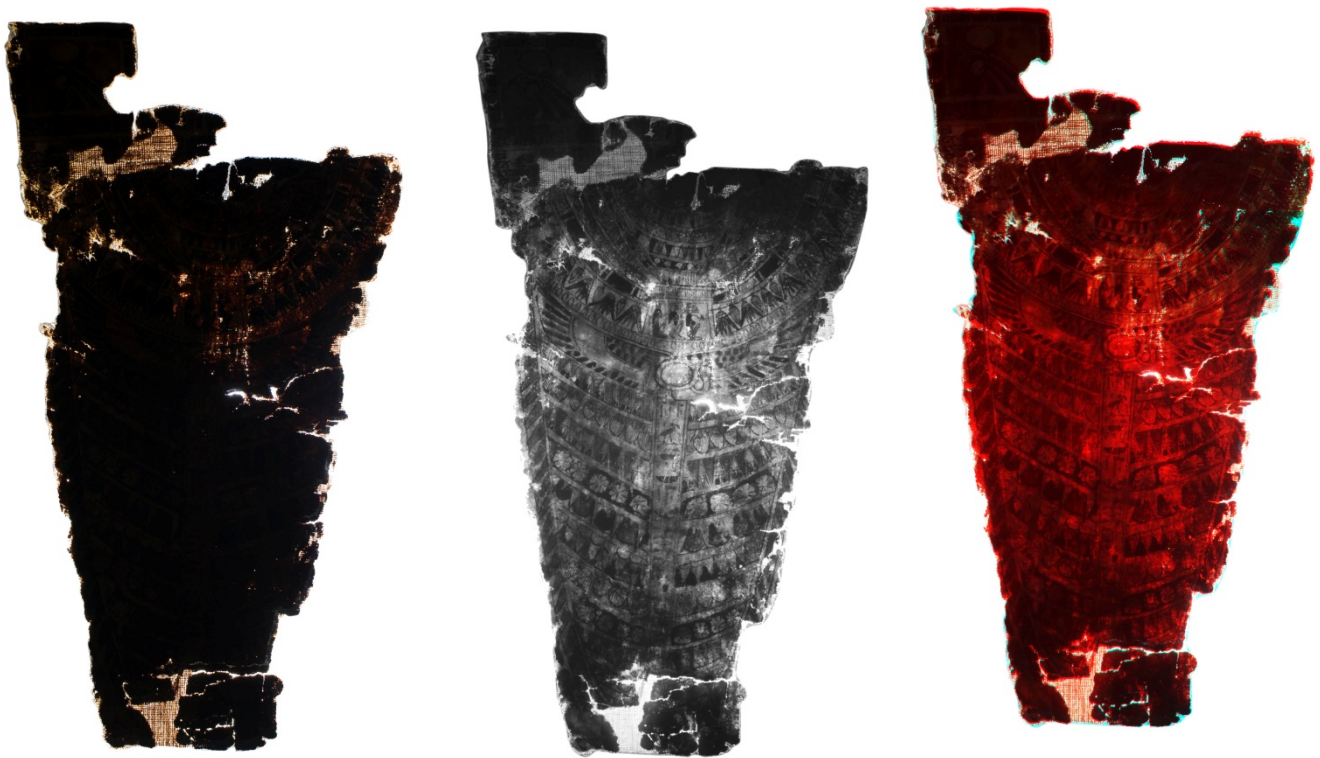


Figure 42. Visible Transmissin - IR Transmitted - IRFC Transmitted.

2.11. Reflectance Transformation Imaging (RTI) (VIS RTI – IR RTI)

This cartonnage presents a number of lines and decorations with pigments and the RTI documentation was carried out in order to test the capabilities of this method as a tool to enhance the details of manufacturing and applying method of the pigments. RTI is a natural way to document painting, since it overcomes the limitation of requiring raking light photography to reveals the decoration lines and method.

In addition to the RGB color, RTI also records the surface normal of each pixel of a scene photographed specially in diffuse gain (Figure. 43 A) filter. These normal are used to render the surface shape of the area but The Specular Enhancement mode (Figure. 43 B) can remove the distracting RGB color from each pixel and provide only the reflectivity.

To understand the next set of images, it is important to understand how to view a normal map. A normal map filter (Figure. 43 C) is a false-color visualization of the direction of the surface normal for a surface. This graphic shows the surface normal map of a sphere. Pixels are shown as pink and magenta are pointing to the right and down, green pixels are pointing up. Variations in the shading depict changes in the direction of the surface normal.

In the RTI images (Figure. 44 a - b), comparing the default and the specular enhancement images allowed uncovering clarified marks relating to surface preparation and tool slips, and give clear vision of the thin areas which shows clearly the texture of the textile.

By using the different filter of RTI and examining the surface of the object, i find that with the use of the diffuse gain filter (Figure. 46), shows the grainy surface of the yellow and red painted layer and shows also inhomogeneous in thickness, most probably due to inadequate preparation of the paint layer and show rough morphology of surface and homogeneous distribution of the blue pigment with many deformation and losses of pictorial layers.

Normal unsharp filter providing more details about the manufacturing technique showing the brush strikes which was crudely applied in different directions especially in the yellow color which applied directly of the white preparation layer (Figure 46 c). Normal visualization filter (Figure. 46 D) reveal the grainy surface of the blue painted layer Its grains were not evenly covered or flow off the brush showing the difference in the thickness from part to another. In

addition, the application of the blue pigment may have been dabbed into place for small areas rather than brushed on in the normal way.

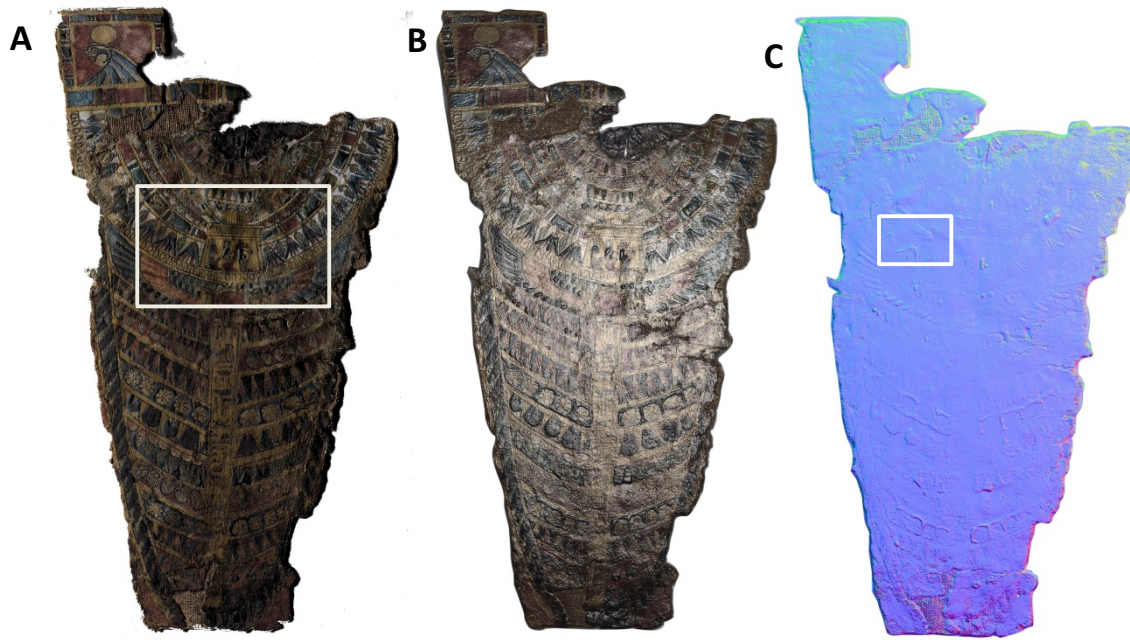


Figure 43. RTI VIS with different filters (Diffuse Gain – Specular Enhancement – Normal Visualization)

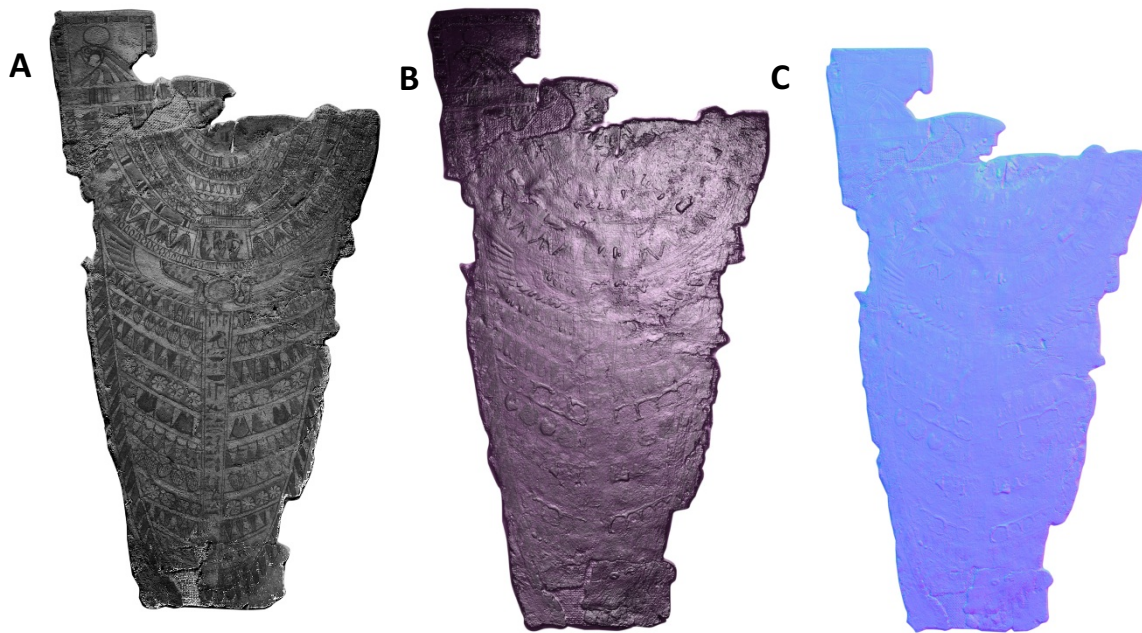


Figure 44. RTI IR with different filters (Diffuse Gain – Specular Enhancement – Normal Visualization).



Figure 45. The diffuse gain filter shows the grainy surface of the yellow layer and the preparation layer.

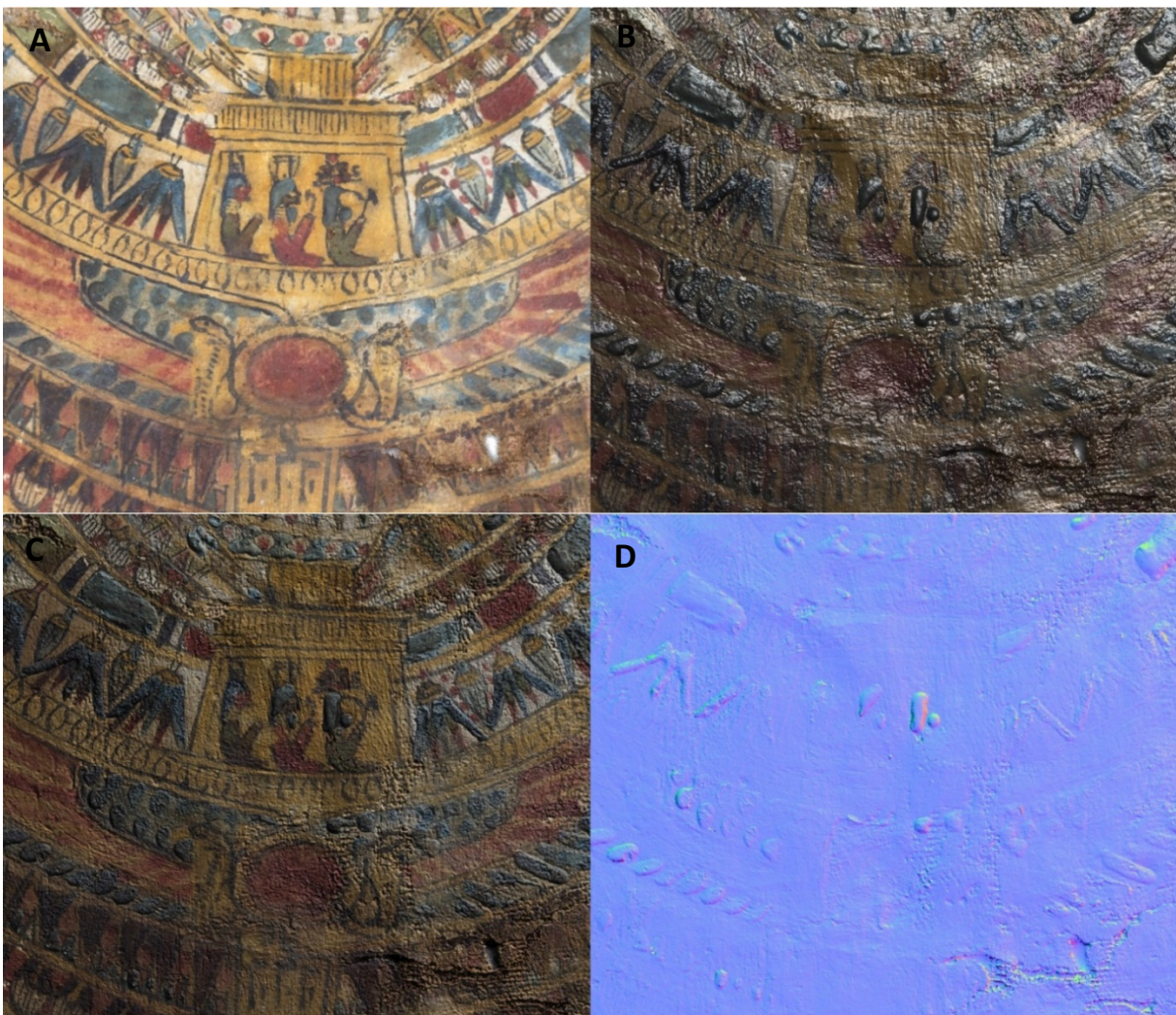


Figure 46. Details with different filters: A: default – B: specular enhancement – C: normal unsharp masking – D: normal visualization

This is the obvious enhancement that the RTI method can provide. It is reasonable to argue that RTI in the infrared range (Figure. 44 A-B-C) can perform an even better documentation with clear details and more information. Infrared light provides more informative RTI images because some pigments, such as red ochre, become transparent; therefore, the photos are not disturbed by the red pigments.

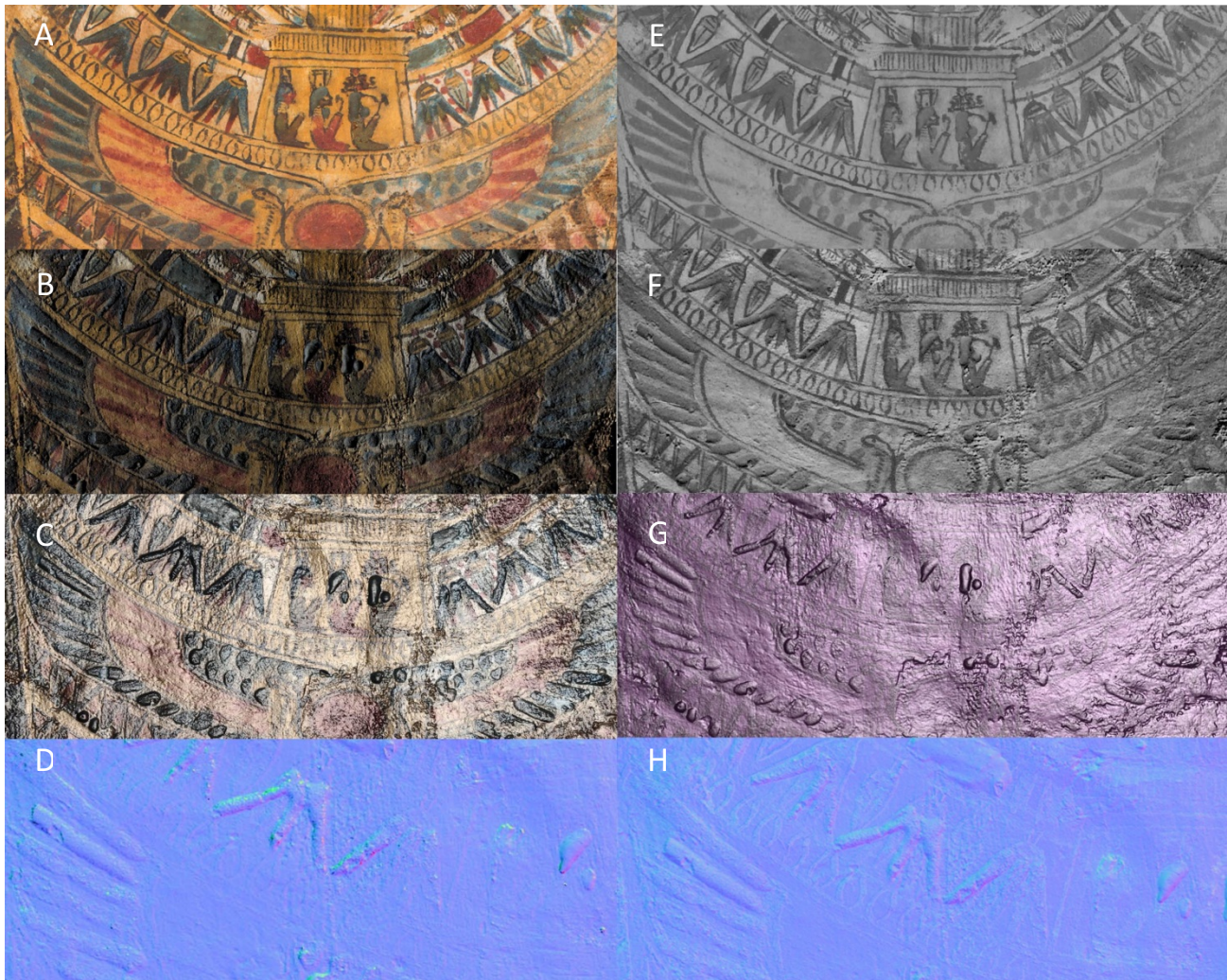


Figure 47. Details with different filters for Visible RTI: A: default – B: Diffuse Gain– C: specular enhancement – D: normal visualization and RTI IR filters E: default – F: Diffuse Gain– G: specular enhancement – H: normal visualization

The object was documented with RTI in the visible (VIS-RTI) (Figure. 43) and infrared (IR-RTI) (Figure. 44) range and they represent different conditions of the surface in some points. In the middle part of cartonnage (Figure. 47 f) shows a series of black lines clear in all the points so it is easily to detect the main lines which used to frame the pigments, which is partially peeled off, thus confusing the detecting of the black lines in visible RGB images.

Some decorated features are not appearing in the Vis RTI normal visualization filter but it appears clearly in IR RTI normal visualization filter. The standard IR photo already provides better documentation of the lines but without showing the thickness of lines or the stratigraphic structure of the pigments (Figure. 47 h).

The comparison of the VIS-RTI and IR-RTI increases the latter for improved detecting of brush direction of applying the preparation layer, traces and evidences. Indeed, while the exclusion of the color information can also be attempted using the diffuse gain parameters, this manipulation of the image is less performing than the IR-RTI, where the result is achieved solely from the infrared photo (Figure.47 f).

In any case, while the color can be eliminated with both modifications, the brightness is still influenced by the paint and so the surface texture is clearer in the IR-RTI than in the VIS-RTI, even with the specular enhancement applied (Figure. 47 c-g).

2.12. X-ray Fluorescence (XRF) Analysis

Eight spots from (Green, Red, Yellow, White, and blue) areas from the surface layer of the Cartonnage were analyzed using (XRF) to obtain information about the pigment identification and to confirm the primary results of Multispectral Imaging.

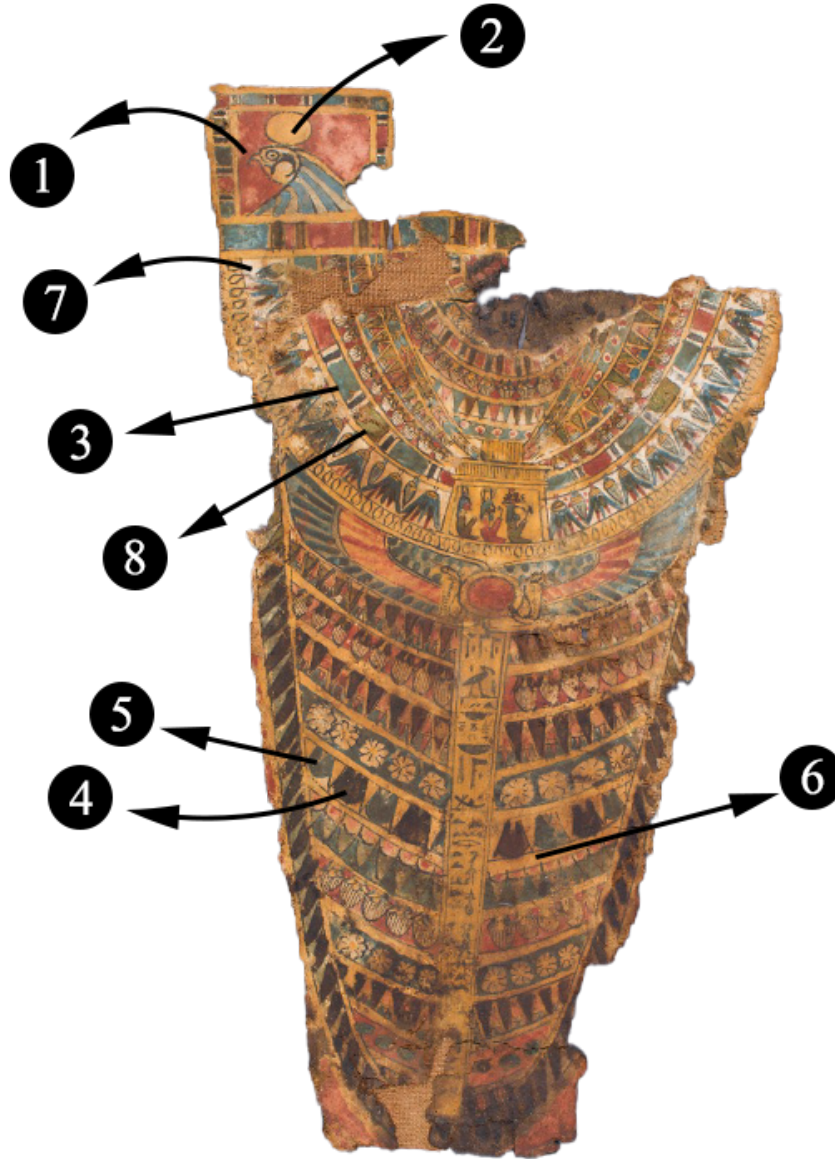


Figure 48. Eight spots of XRF.

2.12.1. Yellow Painted Layer

The result of XRF analysis (Table. 9) showed presence of calcium (Ca), iron (Fe), Sulphur (S), Alumina (Al) and silicon (Si) with traces of Chloric (Cl), phosphor (P) and potassium (K). This result provides evidence for the presence of yellow colorant based pigment that is yellow ochre Iron oxyhydroxide $\text{FeO}(\text{OH})$.

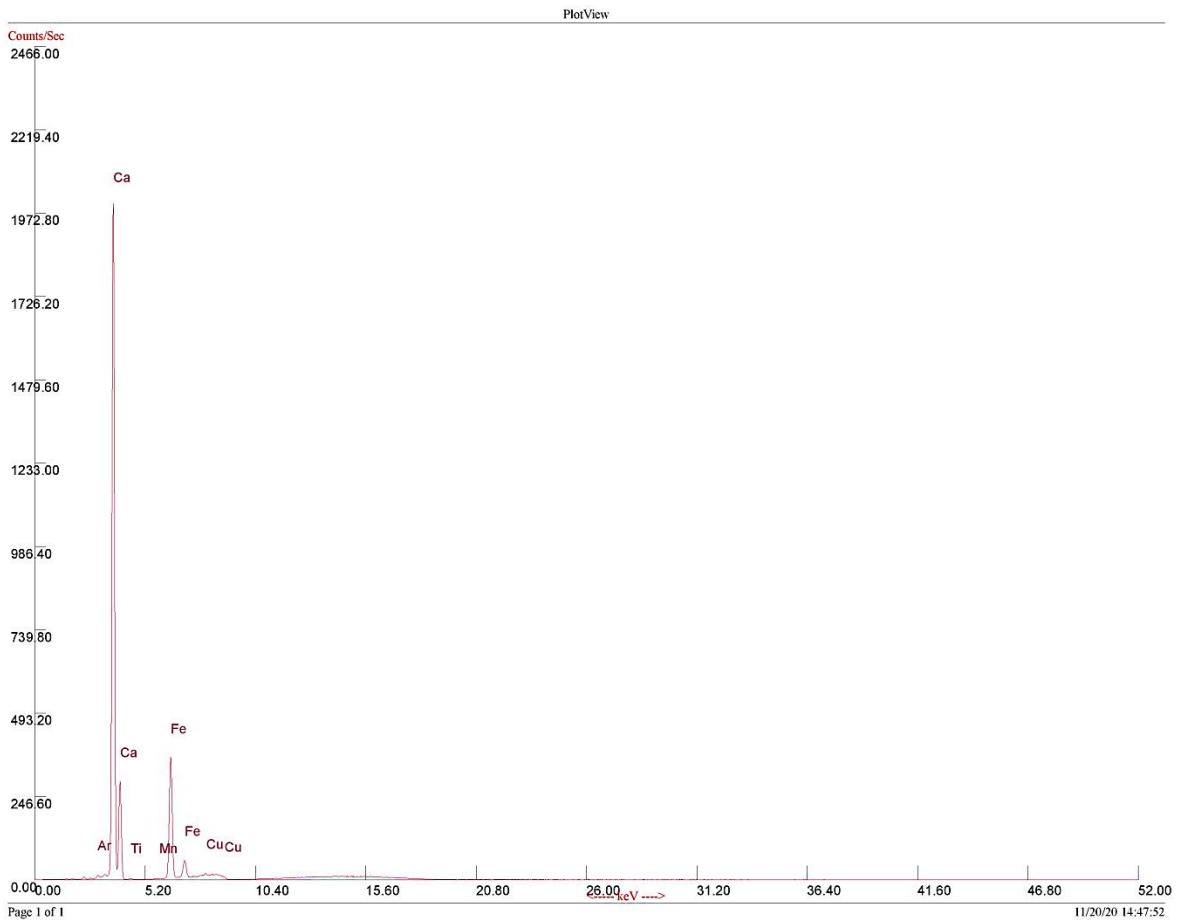


Chart 9. Chart of yellow pigment.

Composition of Yellow Color				
Elements	Area 1		Area 2	
	%	Error	%	Error
Fe	1.208	0.037	0.456	0.024
Ti	0.047	0.008	0.079	0.009
Ca	28.087	0.282	30.854	0.323
K	0.119	0.016	0.081	0.017
Al	0.309	0.085	0.268	0.090
P	0.115	0.018	0.153	0.021
Si	1.138	0.052	1.602	0.062
Cl	0.110	0.003	0.023	0.002
S	1.665	0.030	2.248	0.037

Table 9. The results of X-ray fluorescence (XRF) for the yellow layers.

2.12.2. Blue Painted Layer

According to XRF spectrum of the blue painted layer (Table 10), the elements that presented the highest concentrations were silicon (Si), copper (Cu), and Calcium (Ca). This result provides evidence for the presence of copper-based pigment that is most likely Egyptian blue Calcium copper silicate (CaCuSi₄O₁₀).

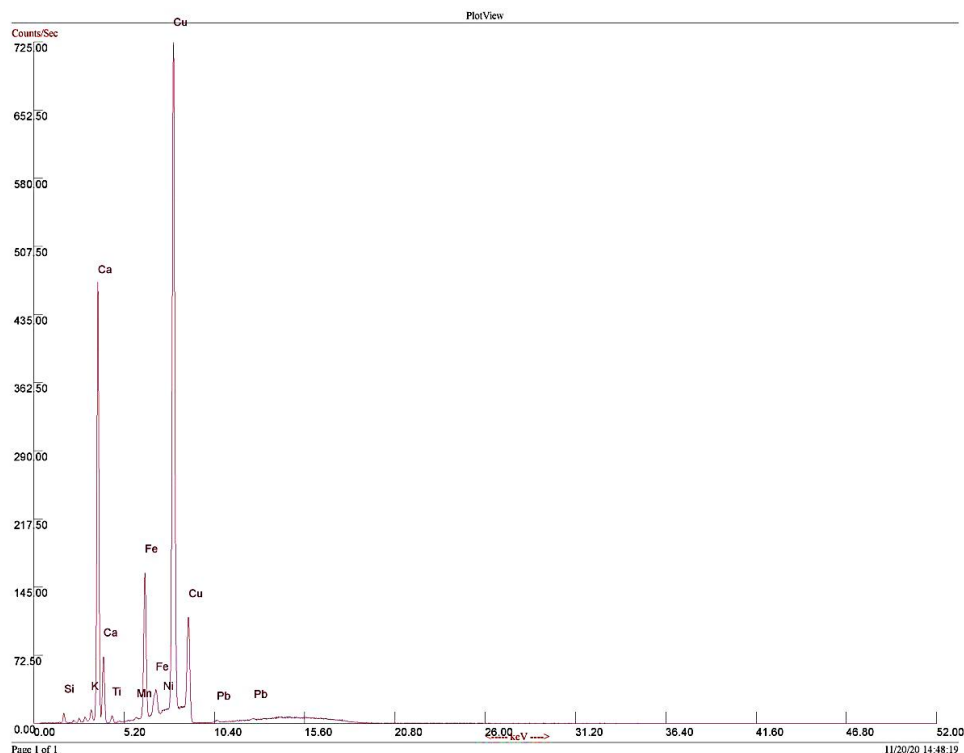


Chart 10. Chart of Blue pigment.

Chapter Four: (Results)

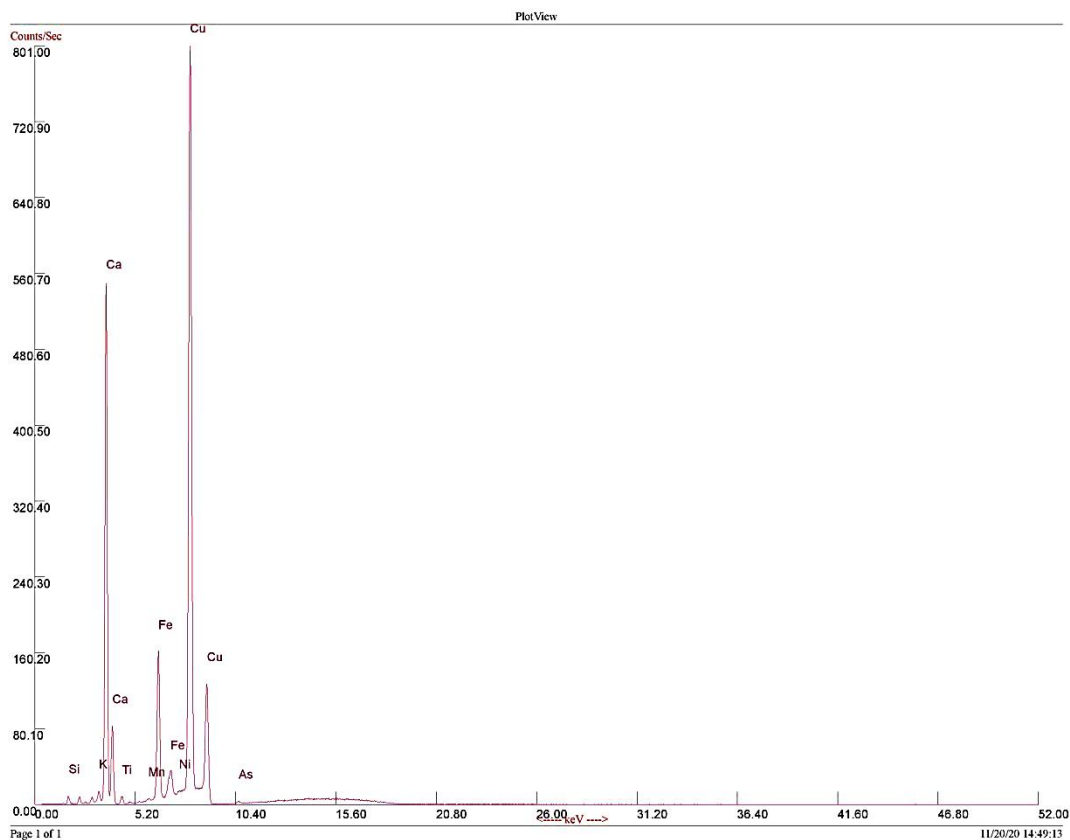


Chart 11. Chart of blue pigment

Composition of Blue Color				
Elements	Area 1		Area 2	
	%	Error	%	Error
Cu	6.243	0.086	6.722	0.091
Fe	0.491	0.021	0.461	0.020
Ti	0.062	0.005	0.063	0.005
Ca	8.709	0.136	9.568	0.141
K	0.319	0.019	0.272	0.018
Al	0.354	0.087	0.466	0.088
Si	13.839	0.185	10.524	0.154
Cl	0.241	0.005	0.092	0.003
S	1.122	0.027	2.523	0.041
P	0.147	0.027	0.207	0.026
Co	0.042	0.008	0.030	0.008

Table 10. The results of X-ray fluorescence (XRF) for the Blue layers.

2.12.3. Green painted layer

From XRF analysis (Table 11), the elements that presented the highest concentrations for some spots on the green painted layer were calcium (Ca) and copper (Cu). This result provides the possibility for the presence of malachite basic copper (II) carbonate $2 \text{CuCO}_3 \cdot \text{Cu}(\text{OH})_2$.

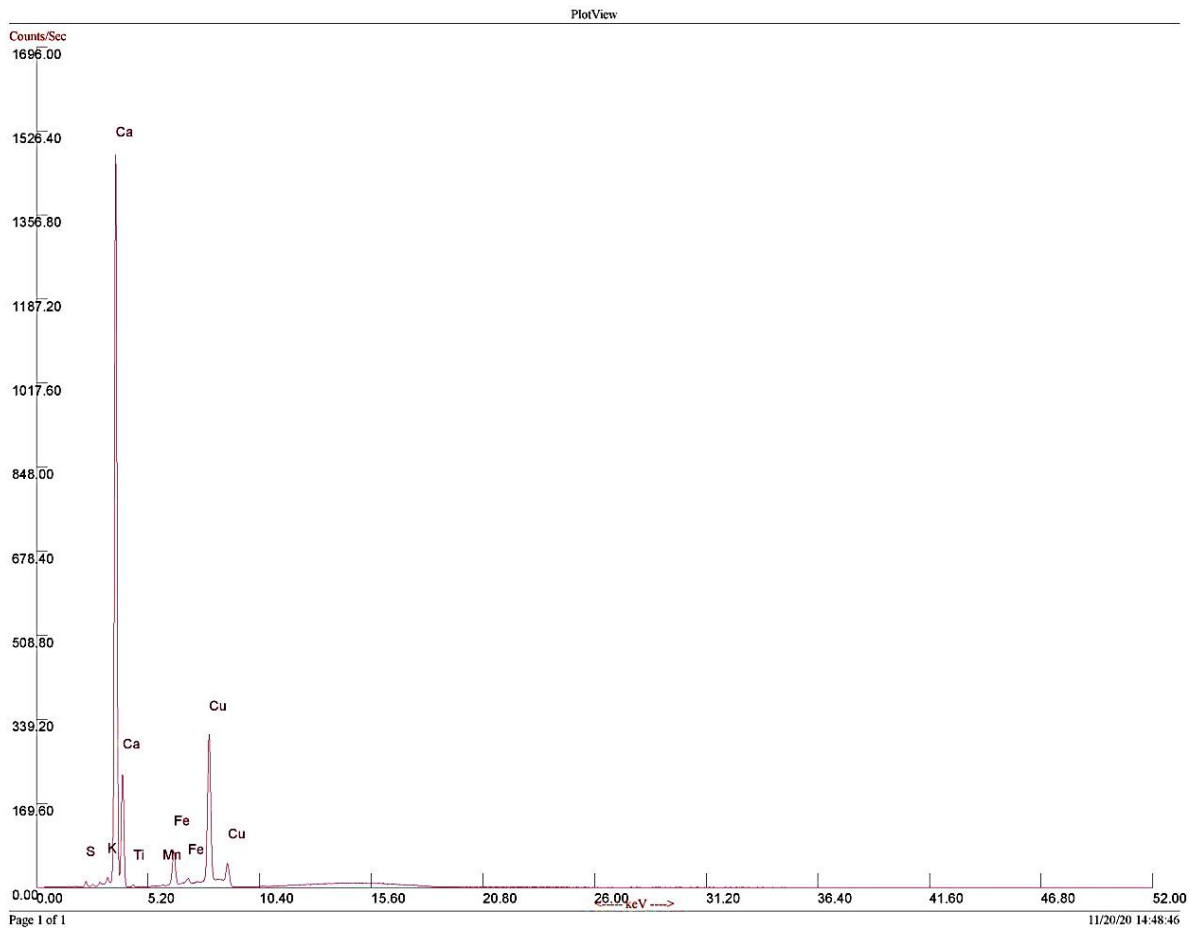


Chart 12. Chart of green pigment.

Composition of Green Color		
Elements	Area 1	
	%	Error
Cu	2.265	0.038
Fe	0.172	0.014
Ti	0.051	0.007
Ca	21.894	0.233
K	0.240	0.018
Al	0.340	0.081
Si	1.664	0.060
Cl	0.194	0.004
S	2.884	0.041
P	0.212	0.022

Table 11. The results of X-ray fluorescence (XRF) for the Green layers.

2.12.4. Red Painted Layer

The result of XRF analysis (Table 12) suggest that the red pigment is red ochre Anhydrous iron (III)-oxide (colored by hematite, Fe_2O_3), consistent with the strong quenching properties of iron-based pigments. The results of XRF analysis for some points on the red painted layer showed presence of calcium (Ca), iron (Fe) and silicon (Si) with a high intensity, in addition to a small amount of sulphur (S) and copper (Cu). This result provides strong evidence for the presence of an iron-based pigment that is most likely hematite Fe_2O_3 .

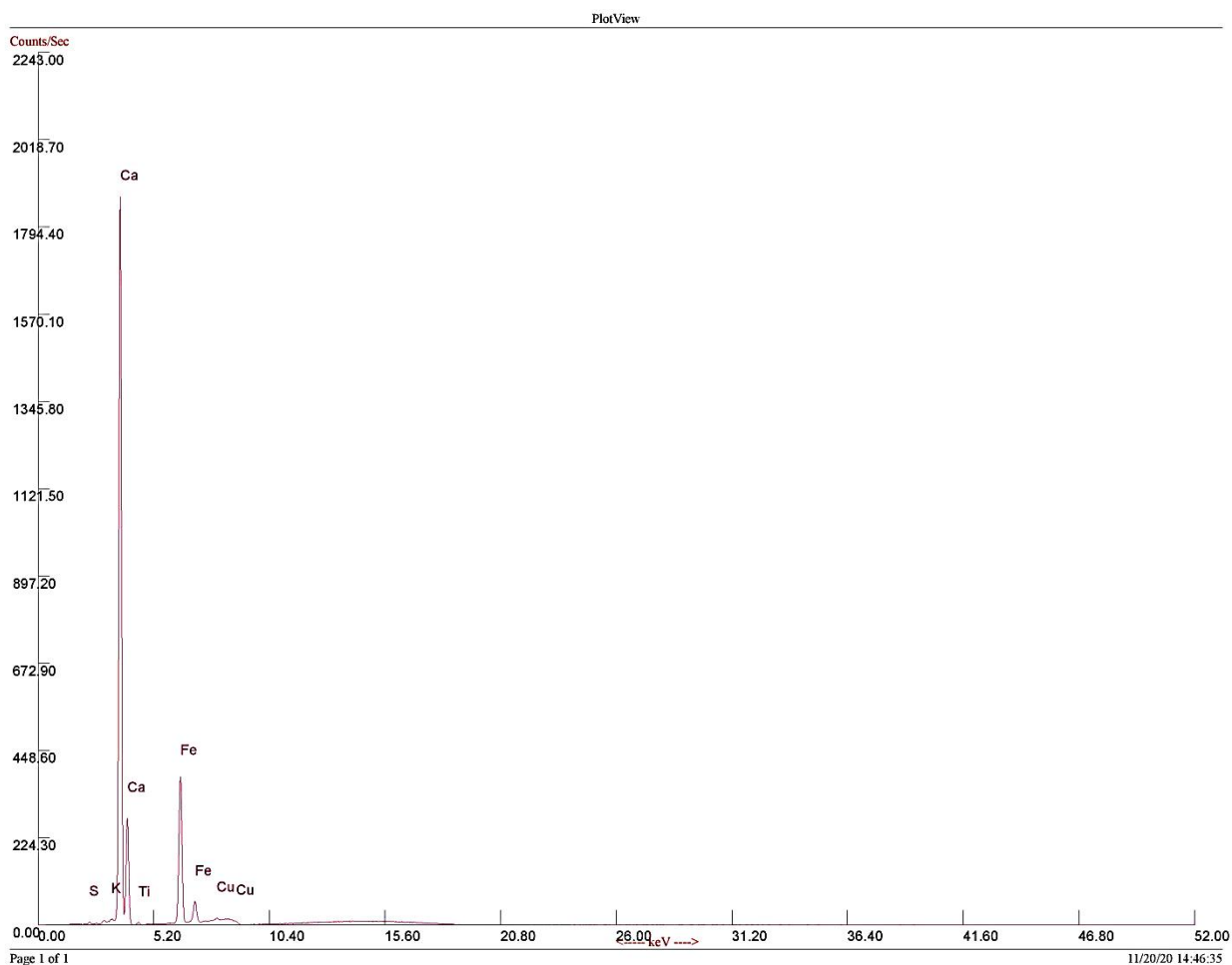


Chart 13. The results of X-ray fluorescence (XRF) for the Red layers.

Composition of Red Color		
Elements	Area 1	
	%	Error
Cu	0.013	0.003
Fe	1.141	0.035
Ti	0.056	0.008
Ca	26.740	0.269
K	0.137	0.016
Al	0.219	0.080
Si	1.925	0.064
Cl	0.099	0.003
S	1.431	0.028
P	0.089	0.018

Table 12. The results of X-ray fluorescence (XRF) for the Red layers.

2.12.5. White Painted Layer

All the XRF spectra, acquired on the surface of the Cartonnage mummy trappings, showed the peaks of calcium and silicon, related to the calcite and quartz in the preparation layer.

Composition of White Color		
Elements	Area 1	
	%	Error
Cu	0.024	0.004
Fe	0.222	0.016
Ti	0.051	0.008
Ca	28.441	0.287
K	0.092	0.016
Si	0.397	0.036
Cl	0.208	0.005
S	0.326	0.015
P	0.106	0.016

Table 13. The results of X-ray fluorescence (XRF) for the white layers.

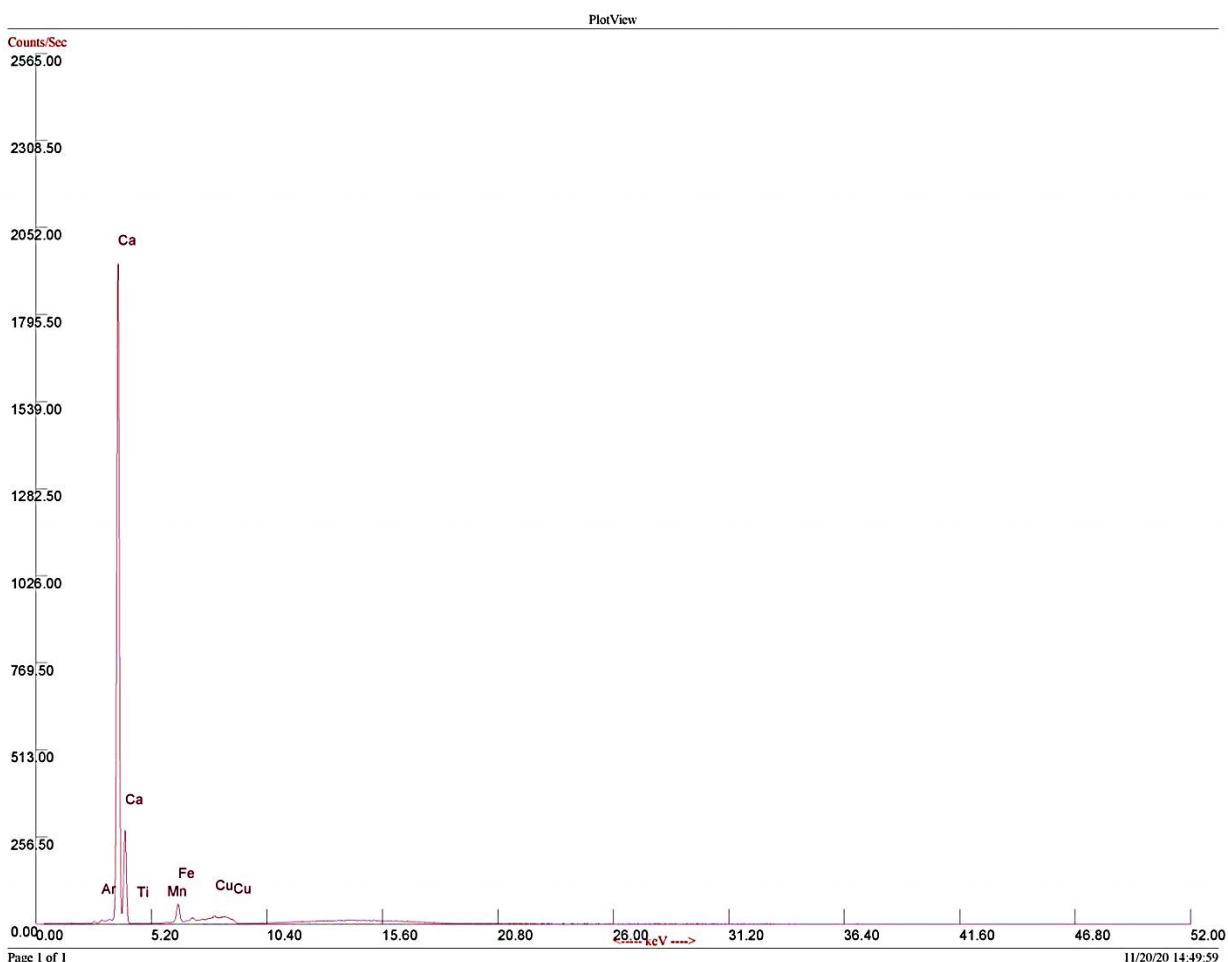


Chart 14. Chart of white layer.

Chapter Five: Discussion

This chapter discussed the results of the multispectral imaging and the X-Ray Fluorescence analysis, to distinguish the pigments and detect the surface characteristic of the two painted objects (wooden coffin and mummy Cartonnage). this discussion with the aim to evaluate the used methods as an effective tool for identifying the ancient Egyptian palette pigments, studying the technique of manufacturing, detecting the strange materials of previous intervention and helping in conservation decision.

The results of multispectral imaging are characterized by being complementary and certain each other's by exposing the two objects to Ultraviolet light and by analyzing the results, ultraviolet fluorescence helped greatly in revealing the authenticity of the surface material and colors and distinguishing between the original color material and the conservation materials and additional touches made due to the different behavior of each material for the (UV) (Figure. 49), recent treatment materials do not fluoresce under (UV) and appear dark but the original varnish and materials often fluoresce under (UV) light. Therefore, there is no doubt that the objects have conserved before and this is apparent in the dark areas of the coffin which confirmed also by Infrared fluorescence (IRF) mapping of blue color and the difference in the color of some pigments on the cartonnage trapping surface which probably because of using consolidation material, the hue fibers spreading on the surface of the cartonnage is evidence that the object was cleaned with cotton swabs and covered with fabric materials which



Figure 49. UV photo shows the conservation materials and additional touches.

attached to the object surface (Figure. 50).

As primary indicators for identifying colors, the MSI is considered one of the methods that help in creating probabilities about the colors used in paintings.

In UVR photo brightness areas were detected and this is indicator for the white color it is gypsum which were used for the preparation layer. XRF spectra of the wooden coffin and Cartonnage mummy trappings, confirmed the using the calcite and quartz in the preparation layer (Figure. 51).

In the green painted layer, the UVF image define that the color could be copper-based pigments because it did not show any fluorescence for the UV light since they are known to quench the fluorescence of surrounding media. Following that Infrared false color images show that the painted green areas appear with a lighter blue hue, which suggests the use of malachite (Figure 52). From XRF analysis, the elements that presented the highest concentrations for some spots on the green painted layer were calcium (Ca) and copper (Cu). This result provides the possibility for the presence of malachite basic copper (II) carbonate $2 \text{CuCO}_3 \cdot \text{Cu}(\text{OH})_2$.



Figure 50. UV photo cotton swabs and the remains of fabric material on the surface of the Cartonnage.



Figure 51. UVR the white color which indicator for gypsum.

By using Microscope for examine the grains of the dark pigment of the cartonnage mummy it shows that it contains grains of green pigments but it framed with dark materials which could be stains or consolidation material used for previous conservation and affect the green color by chemical changes (Figure. 54).

UV photo of the red pigment may be suggested as red ocher (colored by hematite, Fe_2O_3) because of appeared darker in UV consistent with the strong quenching properties of iron-based pigments adding to that the dark appearance in UVRFC and the golden yellow in IRFC photo which outweighs the possibility of being red ocher (Figure. 53).

The results of portable XRF analysis helped in confirming that the red painted layer provides strong evidence for the presence of an iron-based pigment that is most likely red ocher (colored by hematite, Fe_2O_3)

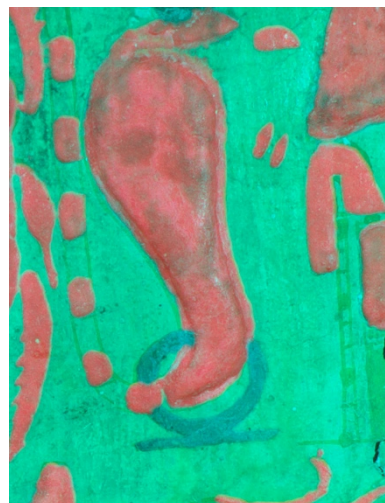


Figure 52. IRFC show the lighter blue and red as indication of malachite and Egyptian blue.



Figure 53. UVRFC, IRFC give indicator for red color.

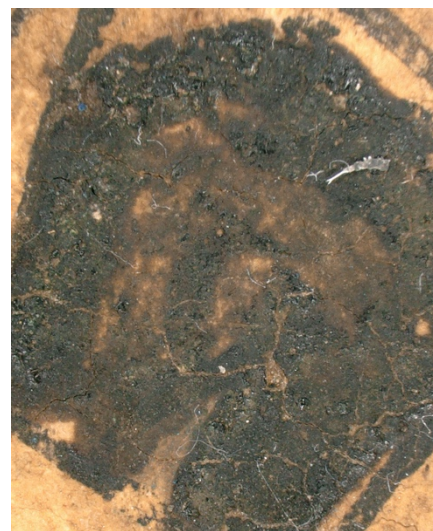


Figure 54. Grains of Green pigments under microscope.

The fluorescence of yellow areas in UVF photo suggests that a yellow-painted layer is probably made of arsenic-based pigments since it gave fluorescent properties and in UVRFC photo yellow color appeared in a purple color and in IRFC appeared greenish yellow.



Figure 55. UVRFC, IRFC give indicator for yellow color.

This is an indication that the yellow color used may be yellow ochre (Figure. 55). The result of portable XRF analysis provides evidence for the presence of two yellow colorants arsenic sulphides based pigment that is possibly orpiment As_2S_3 and yellow ochre Iron oxyhydroxide $FeO(OH)$). That mean the two yellow pigments were used in the ancient Egyptian time and some time they were used for the same object with different in the purpose of use as preparation layer or mixed with Egyptian blue for producing green color or as main color.

In the IRF image, the blue color appeared as bright white indicate the presence of Egyptian blue. IRF photography allows the mapping and detection of Egyptian blue clarifying that the Egyptian blue is the color that has the largest proportion in the objects of this study. Infrared false color image of blue area appeared red, which confirm the presence of Egyptian blue (Figure. 56), XRF spectrum of the blue painted layer, the elements that presented the highest concentrations were silicon (Si), copper (Cu), and Calcium (Ca). This result provides evidence for the presence of copper -based pigment that is most likely Egyptian Blue Calcium copper silicate ($CaCuSi_4O_{10}$).



Figure 56.IRFC , IRF show Egyptian blue mapping.

The black lines and points in UVRFC, and IRFC appear black which may suggest that the black pigment is a carbon-based black, also IR image suggested the presence of carbon based black pigment, which is opaque and in UV photo Black pigments appear darker consistent with the strong absorption properties of carbon. The result of XRF analysis suggest that the black pigment is made from organic materials which not able to detect by the instrument.

The RTI images of The cartonnage object allowed uncovering clarified marks relating to surface preparation and tool slips, and give clear vision of the thin areas which shows clearly the texture of the textile and shows the grainy surface of the yellow and red painted layer and shows also inhomogeneous in thickness, most probably due to inadequate preparation of the paint layer and show rough morphology of surface and homogeneous distribution of the blue pigment with many deformation and losses of pictorial layers (Figure. 57).



Figure 57. RTI photos: left specular enhancement filter, right diffuse gain filter.

The brush strikes which was crudely applied in different directions especially in the yellow color which applied directly on the white preparation layer. Grains of blue painted layer were not evenly covered or flow off the brush showing the difference in the thickness from part to another

(Figure. 57). In addition, the application of the blue pigment may have been dabbed into place for small areas rather than brushed on in the normal way because of the high thickness of some points. IR-RTI shows a series of black lines clear in all the points so it's easily to detect the main lines which used to frame the pigments, which is partially peeled off, thus confusing the detecting of the black lines in visible RGB images (Figure. 58).

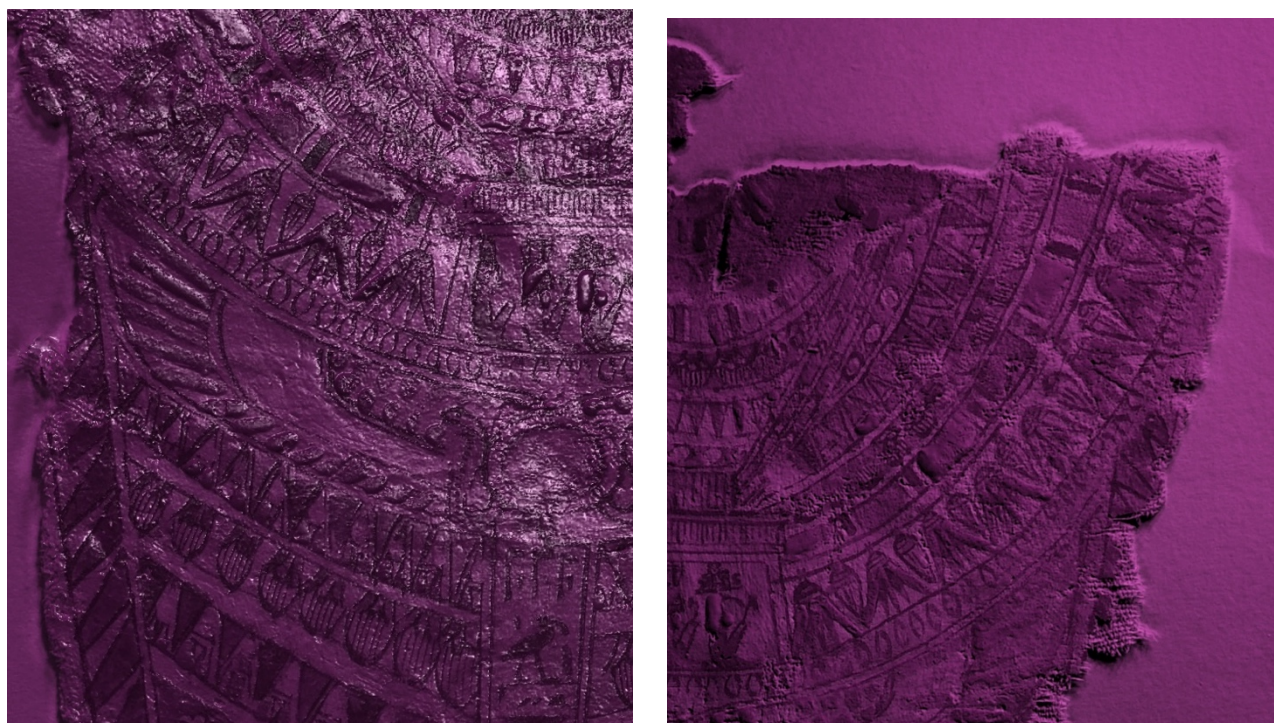


Figure 58. IR RTI: left specular enhancement filter, right diffuse gain filter.

By using RTI on the coffin surface and analyse the photos by changing between different filters of RTI viewer program the sequence of making the structure of painting layer became clear This sequence would start with applying preparation layers on the wood before starting with the actual decoration with marking-out lines, background color, under-drawing, and filling-in of text and decoration with red, blue, and often green. This would be followed by small details in black. The white preparation layer was applied first then the yellow layer as background applied then the red lines colored were applied first, followed by application of the blue figures then the green, and finally details such as eyes and beards of the figures in the vignettes in black. The varnish applied last, on the coffin surface. The sequence of layers and colors determined because of differences in thickness of the layers, which was clear by using RTI technique filters.

Broad brushstrokes in the ground layers are visible and detected in many points of the coffins indicating that the white under-layers have not been burnished before applying the colored decoration. The brush strokes are about 4 cm wide and follow scattered mainly in half circular patterns, just like anybody today would apply a paint coat. The brushstrokes are clearly visible in specular mode because of the use of relatively coarse pigments and a water-based binding medium (mainly gum Arabic). Paint with this combination of materials is not able to form a

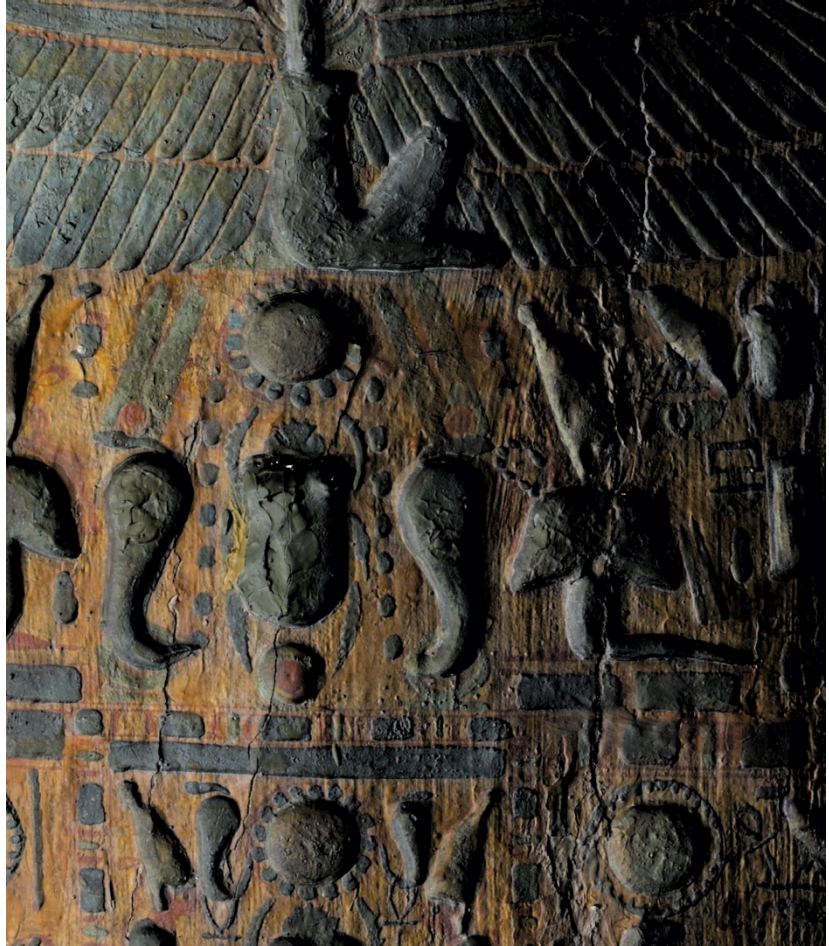


Figure 59. RTI: diffuse gain filter shows the preparation layer texture.

smooth film with drying, and therefore the brush strokes remain visible (Figure. 59).

Finer lines were detected clearly by normal visualization filter in some shapes that's because of tools which used to apply the red and blue sections of the polychrome probably fine brushes and Hollow pens were used. On the coffins underdrawings can be distinguished, either in black or red. Red underdrawings lines are often applied specifically to mark the text bands, either on top or underneath the yellow background layer.

Pastiglia technique has been used for making the scarabs, sun disks and deities in low relief. The Pastiglia has been applied during the white preparation stage the white paste that is used for the preparation was applied to form an organic, round shape with a low relief (Figure. 60). Second method involved making the organic round shapes crisper by edging off the sides, for example with a wooden stick, a flint knife or a piece of metal to have the final shape of figures.



Figure 60. RTI photo specular enhancement show the sequence of adding the figures and pigments.

Chapter Six: Conclusion

The advantages of using a modified “full spectrum” DSLR camera are its low cost and the possibility to use the same camera for other imaging methods, such as technical photography and RTI. The method employs a fairly simple imaging system, but concurrently analyses the data acquired in 3 different modalities: multispectral imaging, reflectance transformation imaging and X-Ray fluorescence. Their advantage over sampling is obvious in reducing the number of samples and also as an affordable and reliable way to extend the achieved results. Non-invasive techniques and evaluation methods have become more accepted than invasive one. However chemical analyses are still needed in some cases.

This research illustrates how the combination of methods developed in the fields of materials sciences, and digital industries can contribute to knowledge exchange as well as the development of new non-invasive ways of studying historical objects. The multispectral imaging system may be used to widen accessibility to equipment, enabling initial investigation of pigments, for example, during preliminary conservation investigations and to identify areas for more detailed analysis.

The use of multiple imaging methods with different light sources have been tried to reach the main goal of the study, which is helped in determining the actual tonal tones of the unknown mummiform cartonnage and painted wood coffin and to achieve maximum benefit and extract information in non-invasive way and avoid the need for samples and secondly to judge the effectiveness of these methods by using simple and inexpensive methods through following approaches and procedures that help In reaching the best result. In the beginning, when the work started, different procedures were followed for each method separately, and this is since each object requires a set of different procedures that are commensurate with his condition.

The coffin photographed by using the panorama method due to the large size of the coffin, which is preferred for getting the high quality which allows the examination in the best way, it to be divided into 4 photos, and then it is assembled.

The method of ultraviolet using UV light was effective and it was found that by increasing the exposure period and moving the LED bulb linearly to the object, the best coverage is

obtained, and thus the best result of the U-V image, through which initial possibilities known about the colors used on the surface of the coffin and the presence on the map of the previous intervention places and helped distinguish between the original colors and the newly added colors.

In addition to that, infrared radiation was used in three ways, the first, IR, and was used in detecting the original lines that were drawn, and the information was monitored smoothly. The procedures that were applied also proved effective and the second method was IRF, which was greatly beneficial in identifying the Egyptian blue also helped reveal the modern touches of the restoration. The third method was IRFC and it was applied according to the procedures followed in most previous studies by mixing IR images with the original image of the antiquity and added confirming information for the Egyptian blue color and exploratory information on the green color. IR transmission image allows us to observe depth aspects of damages such as cracks as well as to show the possibility of visualization of “invisible internal structure” of the painting by comparing individual images to one another. The information from this image could make sure to supply the necessary information to make a plan for actual remedial conservation, especially intervention treatment for reinforcement of deteriorated parts.

RTI documentation was carried out in order to test the capabilities of this method as a tool to enhance the details of manufacturing and applying method of the pigments. RTI is a natural way to document painting, since it overcomes the limitation of requiring raking light photography to reveals the decoration lines and method. RTI provided new and valuable information about the surface condition of the painted layers showing the grainy surface of the pigments and the presence of many deformations and provided also more details about the manufacturing techniques (for example, marks relating to surface preparation and give a clear vision of the thin areas which shows clearly the texture of the textile that was imperceptible to the naked eye or by other inspection techniques).

RTI in the infrared range can perform even better documentation with clear details and more information. Infrared light provides more informative RTI images because some pigments, such as red ochre, become transparent; therefore, the photos are not disturbed by the red pigments. IR-RTI helped to show black lines clear in all the points so it's easy to detect the main lines used to

frame the pigments. The standard IR photo already provides better documentation of the lines but without showing the thickness of lines or the stratigraphic structure of the pigments. IR-RTI increases the latter for improved detecting of brush direction of applying the preparation layer, traces, and evidences. Indeed, while the exclusion of the color information can also be attempted using the diffuse gain parameters, this manipulation of the image is less performing than the IR-RTI, where the result is achieved solely from the infrared photo.

X-ray radiograph was effective and showed the ornamental figures represented by the scarab and the sun, which appeared clearly in a different degree of contrast and details of the deterioration aspects not visible to the naked eye.

The chromatic palette used in the coffin and cartonnage was identified as hematite for the red-painted layer, Egyptian blue for the blue painted layer, possibly orpiment and yellow ochre for the yellow painted layer, Malachite for the green painted layer, and black based carbon for the black painted layer, while a mixture of Egyptian blue and yellow ochre possibly was used for the dark green painted layer.

Using all the information gathered from the multispectral imaging, along with the analysis of XRF of the mummy cartonnage and painted wooden coffin supported the scientific identification of pigments were used in both two objects.

Bibliography

1. ABDRABOU, Ahmed, et al. INVESTIGATION OF AN ANCIENT EGYPTIAN POLYCHROME WOODEN STATUETTE BY IMAGING AND SPECTROSCOPY. *International Journal of Conservation Science*, 2018, 9.1.
2. ALI, Mona F.; DARWISH, Sawsan S.; EL SHEIKHA, Ahmed M. MULTISPECTRAL ANALYSIS AND INVESTIGATION OF OVERLAPPING LAYER CARTONNAGE FRAGMENTS FROM EGYPTIAN MUSEUM, CAIRO. *Scientific Culture*, 2020, 6.3: 25-37.
3. BADR, Nour Mohamed, et al. Identification of materials used in a wooden coffin lid covered with composite layers dating back to the Ptolemaic period in Egypt. *Conservar Património*, 2018, 29.
4. BRUNEL-DUVERGER, Lucile, et al. The contribution of non-invasive and non-destructive techniques to the understanding of the 21st Dynasty Egyptian Yellow Coffins complex stratigraphy: Case of study of E 20043 from the Louvre Museum. *The European Physical Journal Plus*, 2019, 134.6: 257.
5. BURRAFATO, G., et al. ColoRaman project: Raman and fluorescence spectroscopy of oil, tempera and fresco paint pigments. *Journal of Raman Spectroscopy*, 2004, 35.10: 879-886.
6. CALZA, Cristiane, et al. Analysis of sculptures using XRF and X-ray radiography. *Radiation Physics and Chemistry*, 2015, 116: 326-331.
7. CAVALERI, T., et al. A new imaging method of fluorescence induced by multispectral UV for studying historical musical instruments coatings. 2019.
8. CAVALERI, Tiziana, et al. Pictorial materials database: 1200 combinations of pigments, dyes, binders and varnishes designed as a tool for heritage science and conservation. *Applied Physics A*, 2017, 123.6: 419.

Bibliography

9. CHANE, Camille Simon, et al. Integration of 3D and multispectral data for cultural heritage applications: Survey and perspectives. *Image and Vision Computing*, 2013, 31.1: 91-102.
10. COMELLI, Daniela, et al. A portable UV-fluorescence multispectral imaging system for the analysis of painted surfaces. *Review of Scientific Instruments*, 2008, 79.8: 086112.
11. CORREGIDOR, Victoria, et al. Arduino-controlled Reflectance Transformation Imaging to the study of cultural heritage objects. *SN Applied Sciences*, 2020, 2.9: 1-10.
12. CORSINI, Massimiliano, et al. Reflection transformation imaging on larger objects: an alternative method for virtual representations. *BAR INTERNATIONAL SERIES*, 2006, 1568: 407.
13. COSENTINO, A. Multispectral imaging of pigments with a digital camera and 12 interferential filters. *E-Preservation Science*, 2015, 12: 1-7.
14. COSENTINO, A., et al. Panoramic multispectral imaging: training and case studies. *Belgian Association of conservators Bulletin, 2nd Trimester*, 2014, 7-11.
15. COSENTINO, A.; STOUT, S. Photoshop and multispectral imaging for art documentation. *E-Preservation Science*, 2014, 11: 91-98.
16. COSENTINO, Antonino, et al. Multispectral imaging and the art expert. *Spectroscopy Europe*, 2015, 27.2: 6-9.
17. COSENTINO, Antonino. A practical guide to panoramic multispectral imaging. *E-conservation Magazine*, 2013, 25: 64-73.
18. COSENTINO, Antonino. EFFECTS OF DIFFERENT BINDERS ON TECHNICAL PHOTOGRAPHY AND INFRARED REFLECTOGRAPHY OF 54 HISTORICAL PIGMENTS. *International Journal of Conservation Science*, 2015, 6.3.
19. COSENTINO, Antonino. Identification of pigments by multispectral imaging; a flowchart method. *Heritage Science*, 2014, 2.1: 8.

Bibliography

20. COSENTINO, Antonino. Multispectral imaging system using 12 interference filters for mapping pigments. *Conservar Património*, 2015, 21: 25-38.
21. COSENTINO, Antonino. Panoramic, macro and micro multispectral imaging: an affordable system for mapping pigments on artworks. *Journal of Conservation and Museum Studies*, 2015, 13.1.
22. COSENTINO, Antonino. Practical notes on ultraviolet technical photography for art examination. *Conservar Património*, 2015, 21: 53-62.
23. COSENTINO, Antonino. Transmittance spectroscopy and transmitted multispectral imaging to map covered paints. *Conservar Património*, 2016, 24: 37-45.
24. COSENTINO, Antonino; STOUT, Samantha; SCANDURRA, Carmelo. Innovative imaging techniques for examination and documentation of mural paintings and historical graffiti in the catacombs of San Giovanni, Syracuse. *International Journal of Conservation Science*, 2015, 6.1: 23-34.
25. DELANEY, John K., et al. Multispectral imaging of paintings in the infrared to detect and map blue pigments. *Scientific Examination of Art: Modern Techniques in Conservation and Analysis*, 2005, 120-136.
26. DYER, Joanne, et al. A multispectral imaging approach integrated into the study of Late Antique textiles from Egypt. *PloS one*, 2018, 13.10: e0204699.
27. EARL, Graeme, et al. Reflectance transformation imaging systems for ancient documentary artefacts. *Electronic Visualisation and the Arts (EVA 2011)*, 2011, 147-154.
28. EL-RIFAI, Ibrahim, et al. Artwork digitization and investigation a case study of the loom weaver oil painting by Hosni el-Bannani. *Mediterranean Archaeology and Archaeometry*, 2013, 13.2: 21-29.

Bibliography

29. FISCHER, Christian; KAKOULLI, Ioanna. Multispectral and hyperspectral imaging technologies in conservation: current research and potential applications. *Studies in Conservation*, 2006, 51.sup1: 3-16.
30. GIACHETTI, Andrea, et al. A novel framework for highlight reflectance transformation imaging. *Computer Vision and Image Understanding*, 2018, 168: 118-131.
31. GIACOMETTI, Alejandro, et al. Cultural heritage destruction: documenting parchment degradation via multispectral imaging. *Electronic Visualisation and the Arts (EVA 2012)*, 2012, 301-308.
32. HAIN, Miraslov; BARTL, Jn; JACKO, Viado. Multispectral analysis of cultural heritage artefacts. *Measurement Science Review*, 2003, 3.3: 9-12.
33. IMAGING, Cultural Heritage. Reflectance transformation imaging: guide to highlight image capture v2. 0. *Cultural Heritage Imaging, San Francisco, California*, 2013.
34. ISACCO, Enrico; DARRAH, Josephine. The ultraviolet-infrared method of analysis, a scientific approach to the study of Indian miniatures. *Artibus Asiae*, 1993, 470-491.
35. KUBIK, Maria, et al. Hyperspectral imaging: a new technique for the non-invasive study of artworks. *Physical techniques in the study of art, archaeology and cultural heritage*, 2007, 2: 199-259.
36. MAIRINGER, Franz. The infrared examination of paintings. *Radiation in Art and Archeometry Eds. DC Creagh, DA Bradley, Elsevier*, 2000, 40-55.
37. MALZBENDER, Tom; GELB, Dan; WOLTERS, Hans. Polynomial texture maps. In: *Proceedings of the 28th annual conference on Computer graphics and interactive techniques*. 2001. p. 519-528.

38. MANFREDI, Marcello, et al. Measuring changes in cultural heritage objects with Reflectance Transformation Imaging. In: *2013 Digital Heritage International Congress (DigitalHeritage)*. IEEE, 2013. p. 189-192.
39. MANRIQUE TAMAYO, Silvia Noemi; VALCÁRCEL ANDRÉS, Juan Cayetano; OSCA PONS, M^a. Applications of reflectance transformation imaging for documentation and surface analysis in conservation. *International Journal of Conservation Science*, 2013, 4: 535-548.
40. MARENCO, Emilio, et al. Development of a technique based on multi-spectral imaging for monitoring the conservation of cultural heritage objects. *Analytica chimica acta*, 2011, 706.2: 229-237.
41. MUDGE, Mark, et al. Principles and practices of robust photography-based digital imaging techniques for museums. In: *VAST 2010: The 11th International Symposium on Virtual Reality, Archaeology and Cultural Heritage*. 2010.
42. MUDGE, Mark, et al. Reflection Transformation Imaging and Virtual Representations of Coins from the Hospice of the Grand St. Bernard. In: *VAST*. 2005. p. 29-40.
43. MYTUM, Harold; PETERSON, J. R. The application of Reflectance Transformation Imaging (RTI) in historical archaeology. *Historical Archaeology*, 2018, 52.2: 489-503.
44. PALMA, Gianpaolo, et al. Dynamic shading enhancement for reflectance transformation imaging. *Journal on Computing and Cultural Heritage (JOCCH)*, 2010, 3.2: 1-20.
45. PAMART, Anthony, et al. Multispectral photogrammetric data acquisition and processing for wall paintings studies.
46. POUYET, E., et al. 2D X-ray and FTIR micro-analysis of the degradation of cadmium yellow pigment in paintings of Henri Matisse. *Applied Physics A*, 2015, 121.3: 967-980.

Bibliography

47. RE, Alessandro, et al. The importance of tomography studying wooden artefacts: A comparison with radiography in the case of a coffin lid from ancient Egypt. 2016.
48. ROGGE, Corina E.; LOUGH, Krista. Fluorescence Fails: Analysis of UVA-induced Visible Fluorescence and False-color Reflected UVA Images of Tintype Varnishes Do Not Discriminate Between Varnish Materials. *Journal of the American Institute for Conservation*, 2016, 55.2: 138-147.
49. SACKLER, Arthur M., et al. *Scientific examination of art: Modern techniques in conservation and analysis*. 2005.
50. SAMMONS, Jacqueline F. DiBiasie. Application of Reflectance Transformation Imaging (RTI) to the study of ancient graffiti from Herculaneum, Italy. *Journal of Archaeological Science: Reports*, 2018, 17: 184-194.
51. SCHALM, Olivier, et al. Radiography of paintings: limitations of transmission radiography and exploration of emission radiography using phosphor imaging plates. *Studies in Conservation*, 2014, 59.1: 10-23.
52. SCHREINER, M., et al. X-rays in art and archaeology: an overview. *Powder Diffraction*, 2004, 19.1: 3-11.
53. SCHROER, Carla, et al. Accurate Measurement and the Quantification of Surface and Material Property Change Using New RTI and AR Techniques. In: *RATS: Research and Technical Studies Specialty Group Postprints from the 42nd Annual Meeting, San Francisco, CA, May 27 June 1, 2014*. 2014. p. 74-152.
54. SIDDALL, Ruth. Mineral pigments in archaeology: their analysis and the range of available materials. *Minerals*, 2018, 8.5: 201.

Bibliography

55. SITNIK, Robert; KRZESŁOWSKI, Jakub F.; MACZKOWSKI, Grzegorz. Archiving shape and appearance of cultural heritage objects using structured light projection and multispectral imaging. *Optical Engineering*, 2012, 51.2: 021115.
56. STUART, Barbara H. *Analytical techniques in materials conservation*. John Wiley & Sons, 2007.
57. SVOBODA, Marie; CARTWRIGHT, Caroline (ed.). *Mummy Portraits of Roman Egypt: Emerging Research from the APPEAR Project*. Getty Publications, 2020.
58. TOQUE, Jay Arre; SAKATOKU, Yuji; IDE-EKTESSABI, Ari. Pigment identification by analytical imaging using multispectral images. In: *2009 16th IEEE International Conference on Image Processing (ICIP)*. IEEE, 2009. p. 2861-2864.
59. VANDIVERE, Abbie, et al. From ‘Vermeer Illuminated’ to ‘The Girl in the Spotlight’: approaches and methodologies for the scientific (re-) examination of Vermeer’s Girl with a Pearl Earring. *Heritage Science*, 2019, 7.1: 1-14.
60. VANDIVERE, Abbie, et al. Revealing the painterly technique beneath the surface of Vermeer’s Girl with a Pearl Earring using macro-and microscale imaging. *Heritage Science*, 2019, 7.1: 1-16.
61. VANDIVERE, Abbie; WADUM, Jørgen; LEONHARDT, Emilien. The Girl in the Spotlight: Vermeer at work, his materials and techniques in Girl with a Pearl Earring. *Heritage Science*, 2020, 8.1: 1-10.
62. VERHOEVEN, Geert. Imaging the invisible using modified digital still cameras for straightforward and low-cost archaeological near-infrared photography. *Journal of Archaeological Science*, 2008, 35.12: 3087-3100.
63. VERHOEVEN, Geert. Methods of visualisation. In: *Analytical Archaeometry*. 2012. p. 3-48.

Bibliography

64. VERRI, Giovanni, et al. Correction of ultraviolet-induced fluorescence spectra for the examination of polychromy. *Applied Spectroscopy*, 2008, 62.12: 1295-1302.
65. VERRI, Giovanni, et al. Digital mapping of Egyptian blue: conservation implications. *Studies in Conservation*, 2010, 55.sup2: 220-224.
66. WEISS, L. V., et al. The Coffins of the Priests of Amun Egyptian coffins from the 21st Dynasty in the collection of the National Museum of Antiquities in Leiden. 2018.
67. ZHAO, Yonghui, et al. An investigation of multispectral imaging for the mapping of pigments in paintings. In: *Computer image analysis in the study of art*. International Society for Optics and Photonics, 2008. p. 681007.